VARIABLE CAPACITOR BASED MECHANICAL ENERGY-TO-ELECTRICAL ENERGY CONVERTER

A THESIS

SUBMITTED TO THE DEPARTMENT OF ELECTRICAL AND

ELECTRONICS ENGINEERING

AND THE INSTITUTE OF ENGINEERING AND SCIENCES

OF BILKENT UNIVERSITY

IN PARTIAL FULFILLMENT OF THE REQUIREMENTS

FOR THE DEGREE OF

MASTER OF SCIENCE

By

Elif Aydoğdu

August 2007

I certify that I have read this thesis and that in my opinion it is fully adequate, in scope and in quality, as a thesis for the degree of Master of Science.

Prof. Dr. Abdullah Atalar (Supervisor)

I certify that I have read this thesis and that in my opinion it is fully adequate, in scope and in quality, as a thesis for the degree of Master of Science.

Prof. Dr. Hayrettin Köymen

I certify that I have read this thesis and that in my opinion it is fully adequate, in scope and in quality, as a thesis for the degree of Master of Science.

Prof. Dr. Ahmet Oral

Approved for the Institute of Engineering and Sciences:

Prof. Dr. Mehmet Baray
Director of Institute of Engineering and Sciences

ABSTRACT

VARIABLE CAPACITOR BASED MECHANICAL ENERGY-TO-ELECTRICAL ENERGY CONVERTER

Elif Aydoğdu
M.S. in Electrical and Electronics Engineering
Supervisor: Prof. Dr. Abdullah Atalar
and Prof. Dr. Ergin Atalar
August 2007

Today miniature stand-alone systems highly benefit from the improvements in IC technology. Shrinking dimensions to submicron technologies and reduced power consumption in the order of nano-watts open possibilities for new power applications[1–3]. Such systems demand integrated, long lasting micro energy sources, and at that power level, ambient energy scavenging arises as an alternative solution, as energy harvesting units can be integrated conveniently through MEMS(micro electromechanical systems) technology.

This thesis offers one such solution. A novel generator design with electrostatic approach is presented. The generator creates new electrical charge, thus it can be used to recharge a reservoir. It is composed of variable capacitors and switches. As it does not employ inductive components, it is suitable for environments in which magnetic fields should be avoided. Throughout the thesis the design is further improved to overcome the restriction on the achievable electrostatic field given the dimensions and voltage level. A third electret with permanent charge is embedded in between the plates of the capacitor creating

extra field inside the capacitor at the same potential. On the mechanical side, more work is done against increased electrostatic force; and on the electrical side more charge accumulation and a greater charge gain is achieved.

The system is simulated using PSpice and the results are consistent with the theoretical expectations. An experiment utilizing macro elements is also carried out with 81% efficiency; when source voltage is 40V, frequency is 1Hz, and $C_{max} = 1500$pF the power gain is 880nW. For micro applications 1500pF is achievable, but 40V is very high; so lower voltage sources should be used and power gain will be much smaller. The electret idea may solve this problem, and one other considerable solution is to increase the maximum capacitance. For the future, our purpose is to reach higher capacitance in limited volumes through new capacitor designs and making use of microfluidics technology.

Keywords: Self-powered systems, mechanical-to-electrical energy conversion, electrostatic energy conversion, variable capacitors.

ÖZET

ORTAMDAKİ MEKANİK ENERJİYİ ELEKTRİK ENERJİSİNE ÇEVİREN KAPASİTÖR TABANLI DEVRE TASARIMI

Elif Aydoğdu
Elektrik ve Elektronik Mühendisliği Bölümü Yüksek Lisans
Tez Yöneticisi: Prof. Dr. Abdullah Atalar
ve Prof. Dr. Ergin Atalar
Ağustos 2007

Günümüzde minyatür bağımsız sistemler entegre devre teknolojisindeki ilerlemelerden büyük ölçüde faydalanmaktadırlar. Micronaltı teknolojilere ulaşan boyutlar ve nanowattlara düşen güç tüketimi, yeni besleme uygulamalarına imkan tanımaktadır. Bu gibi sistemler entegre, uzun ömürlü mikro enerji kaynaklarına ihtiyaç duyarlar ve bu noktada, ortam enerjisini kullanma fikri iyi bir alternatif oluşturmaktadır. Mikroelektromekanik sistemler (MEMS) teknolojisi, enerji dönüştürücüleri tümleşik devrelerle aynı yongalar üzerine üretebilmektedir.

Bu tezde ortamdaki mekanik enerjiyi elektrik enerjisine çeviren yeni bir kapasitif devre tasarımı sunulmaktadır. Tasarım elektriksel yük üretebilmekte, dolayısıyla bir kaynağı yükleyebilmektedir. Değişken kapasitörlerden ve anahtarlardan oluşan tasarım endüktif elemanlar içermemektedir ve bu yönüyle manyetik etkilerden sakınılması gerekenler ortamlar için de uygundur. Ayrıca bu tasarım alan ve voltaja bağlı elektrostatik alan kısıtlamalarına karşı daha da geliştirilmiş, kapasitör plakaları arasına sabit yük tutan ve içeride ilave elektrik alan oluşturan üçüncü bir elektret yerleştirilmiştir. Mekanik anlamda artan elektrostatik

kuvvete karşı daha çok iş yapılmakta, elektrik anlamda da daha çok yük birikimi sağlanmakta ve daha yüksek yük kazancına erişilmektedir.

Sistem PSpice kullanılarak modellenmiş ve teorik hesaplamalarla tutarlı sonuçlar elde edilmiştir. Makro elemanlarla oluşturulan bir deneyde de %81 verim elde edilmistir. Bu deneyde 40V enerji kaynağı ve 1500pF'lık iki kapasitör kullanılmış, 1Hz'lik operasyonda 880nW güç kazancı sağlanmıştır. Mikro uygulamalarda da 1500pF kapasitansa ulaşılabilir, ancak 40V oldukça yüksek bir değer olup yerine çok daha düşük güç kaynakları kullanılmalıdır ve bu da enerji kazancının daha az olacağı anlamına gelir. Elektret kullanma fikri düşük enerji problemine bir çözüm oluşturmaktadır, bir başka etkin çözüm de kapasitans değerini artırmaktır. Gelecek için hedefimiz kısıtlı bir alan içerisinde daha yüksek kapasitans değerlerine ulaşabilecek yeni kapasitör tasarımları oluşturmak, bunun için de mikroakışkanlar teknolojisi gibi yeni yöntemlerden faydalanmaktır.

Anahtar kelimeler: Kendi gücünü sağlayan sistemler, mekanik-elektrik enerji dönüşümü, elektrostatik enerji dönüşümü, değişken kapasitörler.

ACKNOWLEDGEMENTS

It was great chance and pleasure for me to work with two excellent advisors, professors Abdullah Atalar and Ergin Atalar. I am grateful for all the knowledge, experience and great perspective they shared with me. They are special advisors, motivating their students in worst days with their optimism, and trust. I am really proud of being their student.

I am thankful to Hayrettin Koymen, and Ahmet Oral. They kindly helped me to finish up my thesis and enriched my work sparing their valuable time.

Next comes my colleagues Erdem, Makbule and Ozlem; thank you for all your valuable effort that helped me through this rocky road; and Selim and Niyazi, without you I would have already ran away, your patient guidance taught me much, thank you my ulterior advisors; and finally all the members of Bilkent Biomedical Engineering Group, your appreciation and courage in those pizza meetings motivated me a lot, hope you all get your degrees seamlessly.

EA229 was like a home with a family inside, thank you Celal abi, Erdinc, Makbule, Emre, Can, Ugur (Cuma), and also Esra, Kivanc and all other graduate and undergraduates; my research was going much faster(!) with endless conversations!

I kindly appreciate every piece of knowledge from all my instructors in undergraduate and graduate study, and I especially thank Ergun abi, Ersin abi and Muruvet abla for their generous help.

And finally, my whole big kind-hearted family, the energy of each of your love standing by me cannot be appreciated enough in any ways, but you all know that I love you much.

Contents

List of Figures

Chapter 1

INTRODUCTION

The rapid progress in integrated circuit (IC) technology lowered the power required by the systems so drastically that it may be plausible to provide mobile power by means other than a battery. This progress, which in turn means shrinkage in dimension, requires the power supply to get smaller and even be integrated to the rest of the circuit when the interconnections, electronic noise and control complexity are considered. As a solution, integrated chemical batteries may be improved, but the shelf life and replacement accessibility arise as a limiting factor especially in medical and wireless sensor-actuator applications. At that point self-powered-system designs harvesting the environmental energy can emerge as smart alternatives. It may be possible to feed small stand-alone systems through continuous energy scavenging from the environment by means of an integrated energy conversion unit. The MEMS technology which improves in parallel with IC industry is the enabling tool for integrating the energy harvesting methods on the same chip with the functional electrical circuits.

1.1 Mechanical-to-Electrical Energy Conversion Mechanisms

One strategy of building a self-powered system is to harvest the required electrical energy from the ambient mechanical energy, which manifests itself mostly in vibrational form. Towards this direction, various kinds of generators (energy converters) have been devised as discussed in [4, 5]. A class of such generators capture the ambient mechanical energy through induced motion of movable plates of capacitors and use it against the electrostatic force [6–9]. Another work is on exploiting magnetic effects and in particular Faraday's law of induction after the conventional large scale generators [10, 11]. Yet another class relies on piezoelectric effects where ambient mechanical energy sustains a pressure field on the piezoelectric material [12, 13]. Electromagnetic and piezoelectric converters can give power output at the order of $\mathrm{mW/cm^3}$, while this value is at most $100\mu\mathrm{W/cm^3}$ for electrostatic converters; but although it gives the lowest power output, our choice is electrostatic (capacitive) energy generation due to MEMS compatibility of such designs, and ease of manufacture. In addition, electrostatic power generators can function in high static and electromagnetic fields.

1.2 Electrostatic Energy Generation

Electrostatic energy generation is based on electrostatic field alteration under the effect of physical force. Work done by the mechanical force opposing the electrostatic force is transformed into electrical energy. Circuitry of such a system involves variable capacitors, physical attributes of which can be varied by mechanical energy; and control and energy transfer elements.

The main advantage of generators that employ only variable capacitors is that they can be manufactured completely in MEMS processes where the building

material is pure silicon. On the other hand, most of the designs that make use merely of variable capacitors proposed so far have a major disadvantage: unless an inductor is included, they can not be used to recharge a single battery, or a reservoir, because they do not produce charge. The associated mechanism for each generation cycle is to deliver an amount of charge picked from the reservoir to a load at a voltage higher than that could be provided by the reservoir itself [8]. A different design makes use of the current resulting from the charge between a fixed value capacitor and a variable capacitor potential of which fluctuates as its capacitance is mechanically altered [7]. In this design, it is assumed that the initially embedded charge which is flowing between the capacitors is constant without any leakage, but actually it will leak through the capacitors as time passes and in order to keep the energy gain constant in time this charge should be periodically replenished by an external source. These designs are incapable of producing new charge, they can only take the charge from one reservoir and charge another reservoir with a larger voltage. If an inductor is included to the design, the required inductance value is so high that it is impossible to integrate it on a single chip [6,9]. In many cases, an external inductor is not very desirable because of the increase in required space and also difficulties in manufacturing process. On the other hand, our generator consists of only variable capacitors and switches and it can produce new charge. Hence, it can be used to store electrical power to a reservoir for further use, while it can easily be manufactured fully in an integrated form. The same design is patented by Gimlan in 2005 [14], but he did not prove its functionality through theoretical analysis or simulations.

The energy gain of all the electrostatic designs converge to the maximum energy of the variable capacitor, $0.5\ C_{max}\ V^2$, and power gain is determined together with frequency of operation, $0.5\ C_{max}\ V^2\ f$. So, the power gain of an electrostatic system varies depending on the variable capacitor design and the application frequency. For body implant applications the frequency of input mechanical motion is very low, in the order of Hz, but for other applications it

may rise up to KHz level. In the literature some achieved power values are as follows; converter of [6] works at 2.5 KHz and 3.6μW/cm^3 power gain is expected, converter of [29] works at 50Hz giving 120nW power output at 21% efficiency, converter of [7] is simulated at 1.2KHz giving 100μW power, and converter of [9] is expected to work at 10Hz with 24μW power output (for the last three converters exact dimensions are not mentioned). On the other side, the power consumption of a micropower programmable DSP [3] is 560nW, a pacemaker is 60μW, and a watch is 5μW which all seem to be achievable.

In the subsequent chapter, following a discussion of the theory of the generator, we provide SPICE simulation results of the electrical behavior of the design and an experiment. In the third chapter, an improvement on the design is suggested together with the theoretical analysis and SPICE simulations. The fourth chapter discusses the implementation considerations including mechanical design issues, restrictions on physical parameters and fabrication constraints; summary and discussions follow in the conclusion chapter.

Chapter 2

SWITCHED-CAPACITOR ENERGY CONVERTER

2.1 Introduction: Capacitor as an Energy Converter

Mechanical-to-electrical energy conversion can be accomplished through an electrical component, energy of which can be increased by altering its physical parameters under the effect of mechanical force. Capacitor, inductor and piezoelectric materials are such components. Among those, capacitor is the most suitable one for micro-scale applications as it is easily fabricated in a MEMS process. So, we focused on capacitive energy conversion, as the aim is to come up with an energy unit integrated in an IC.

Voltage on a parallel plate capacitor is related to charge with the equation,

$$q = C\ V \tag{2.1}$$
$$V = \frac{q\ d}{\epsilon\ A}$$

where d is the distance between the plates of the capacitor, q is the amount of charge on each of the plates, A is the area of the plates and ϵ is the permittivity of the dielectric between the plates. While the capacitor is at a fixed state with nonzero charge on it, if we increase d, or decrease ϵ or A this will increase the voltage —and the energy stored on the capacitor. So, any applied mechanical force working against the electrostatic force between the plates, alters one of these parameters raising the electrical energy. The design presented in this thesis aims to convert the energy increase on a capacitor into charge accumulation in the system.

The basic idea of our design is to use more than one capacitor and make use of all the charge induced at the plates of the capacitors in serial connection. The circuit will consist of an electrical energy storage unit (reservoir) which supplies the initial charge for the capacitors and receives the harvested energy; and a mechanical energy harvesting system utilizing variable capacitors together with switches that are capable of uniting the capacitors either in series or in parallel configuration. When the switches are properly operated in synchrony with the motion of the capacitor plates, the system charges the reservoir.

This sort of circuitry is familiar from charge pumps that rely on switching between serial and parallel connected capacitor configurations [17–19]. However, the operation principle is actually the dual —or inverse— of what is done in charge pump circuits. Charge pumps raise the potential to high levels making use of switching, while this system sacrifices potential difference in return for extra charge and compensate the potential drop through use of mechanical energy input.

The aim is to charge the capacitors up with the highest amount of charge possible while they are in serial connection (Figure 2.1a), and then separate the capacitors —keeping the charge on their plates— to connect them in parallel (Figure 2.1b). This way, at the terminals of the composite structure we will

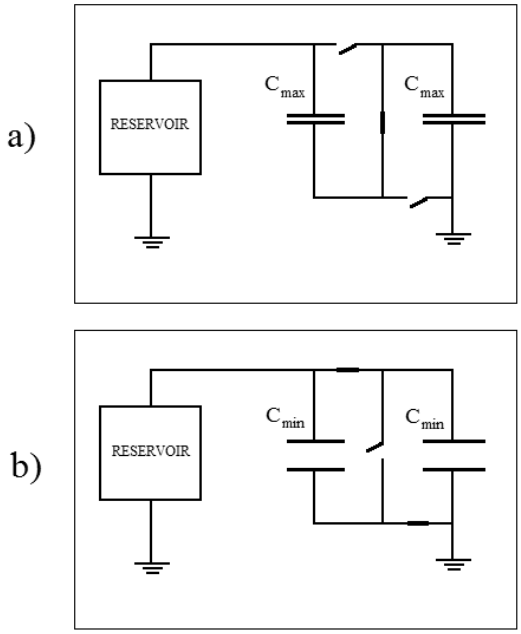

Figure 2.1: Circuit diagram of a two capacitor energy harvesting system. It consists of variable capacitors and switches that connect the capacitors either in serial as in (a) or in parallel as in (b).

have n (number of capacitors) times the amount of charge we had when they were serially connected, meaning a gain in charge. This increased amount of charge should be sent to the reservoir. To do this large enough potential should be maintained on the capacitors to pump greater amount of charge back to the reservoir. This is achieved through use of mechanical energy that decreases the capacitance; capacitors discharge to the reservoir until their capacitance reaches minimum value. As long as $C_{max} > \frac{n^2}{n-1} C_{min}$, this system gives back more charge than it took and there is a net charge gain in every cycle.

2.2 Application Of The Principle

The development of the circuit design can be divided into two stages. The initial design employs n variable capacitors, $n-1$ switches for connecting capacitors in series, $2(n-1)$ switches for connecting capacitors in parallel; and these switches are controlled via a feedback circuitry that synchronizes the switch operation to

mechanical motion. A second design evolved, as it was realized that the switches can be replaced with diodes.

The most advantageous design in the sense of fabrication, operation and efficiency is the second design, as it employs only diodes in addition to variable capacitors and there is no need for any feedback control circuitry. Going through a brief description of the earlier stage in this section, in the next section the final design will be explained in detail with supporting analysis, simulation and experimental data.

2.2.1 Feedback-Controlled Energy Converter Design

The first attempt towards implementation was direct application of the idea "charge while capacitor energy decreases, discharge while capacitor energy increases". So the initial design utilizes switches (which can be MOSFET or other transistors) that are controlled through an external signal that gets feedback from the circuit to know the phase of the capacitor motion. Diagram of such a circuit is given in Figure 2.2. The control signals S1 and S2, one controlling serial connections and the other controlling parallel connections, turn the serialization switches on and parallelization switches off while capacitance increases, and they turn the serialization switch off and parallelization switches on while capacitance decreases as given in the sinusoidally varying capacitance case in Figure 2.3. This way, they discharge in parallel connection while mechanical energy is captured by the system and they are charged up in serial connection.

The disadvantage of this design is that an additional circuitry is needed for control purposes, which consumes a part of harvested energy. Also this external control may cause mismatch in timing which will in turn cause a loss in energy conversion efficiency.

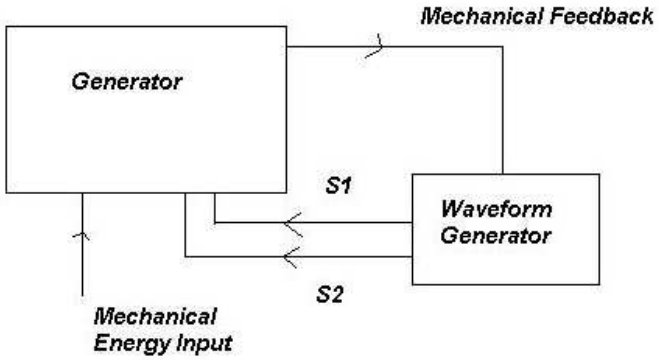

Figure 2.2: Feedback-Controlled Energy Converter Model.

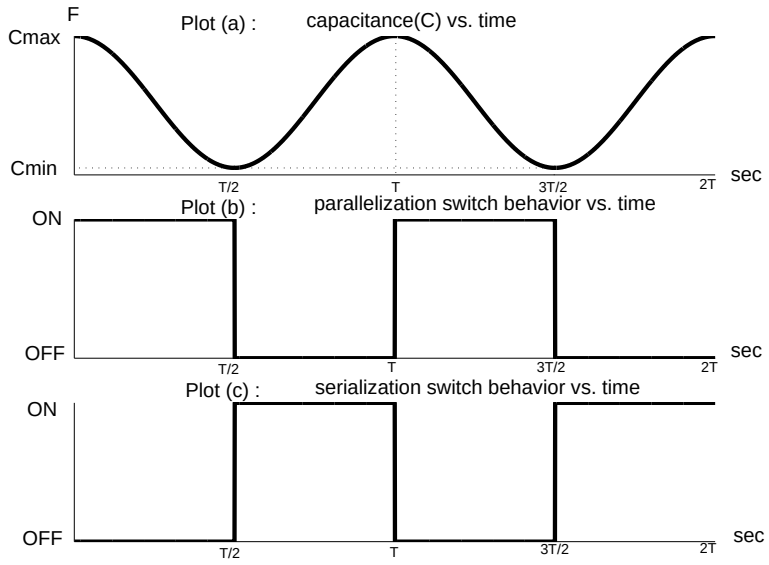

Figure 2.3: Time plots of the switch behaviors relative to the capacitor motion which is sinusoidal in this case.

2.2.2 Self-Controlled Energy Converter Design

The simpler and better implementation of the idea utilizes diodes substituting the switches. There exist $3(n-1)$ diodes each replacing one of the switches. There are two main paths for current in this configuration. When current tends to flow out of reservoir it has to pass through the diode connecting the capacitors in serial, and when it tends to flow into the reservoir it has to pass through the diodes connecting the capacitors in parallel. So, the reservoir delivers charge to capacitors in serial connection and receives charge in parallel connection.

Figure 2.4 shows the positions of the diodes in the circuit model for two capacitor case: D_1 and D_3 (which serve as the parallelization switches) let the current flow in the C_2 - reservoir direction which enables parallel connection when the capacitors start to capture external energy and their potentials are forced to raise. This way the energy is transferred to the reservoir by charging it up. D_2 (the serialization switch) enables serial connection by letting current flow from the negative terminal of C_1 to the positive terminal of C_2 when the capacitor potentials are forced to decrease and this way the reservoir charges the capacitors up. There exists a continuous charge transfer between the capacitors and the voltage source to compensate for the capacitance changes.

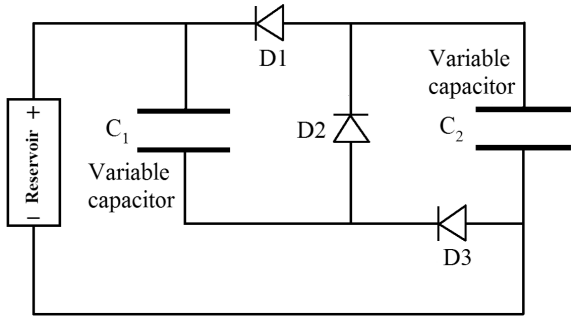

Figure 2.4: Self-controlled energy converter model, utilizing diodes in place of switches.

The reservoir of this circuit can be either a voltage source or simply a capacitor. These two cases are separately analyzed in the following sections. For both cases two-capacitor models are used for convenience.

2.3 Self-Controlled Energy Converter Design Utilizing Voltage Source

For the case a voltage source is used as the reservoir, the equivalent capacitor formed by either parallel or serial connected capacitors has the same potential with reservoir, V on it all the time. Whenever mechanical variation forces the

potential on the capacitors to get larger or smaller than V, a charge transfer occurs between the source and the capacitors, to balance out the potential difference. The following is the analysis of the charge transfer behavior during a full cycle of operation. We calculate the amount of charge gain and converted energy.

The values of C_1 and C_2 will be assumed to be exactly equal to each other and will be referred as C. The voltage applied by the voltage source is represented by V. It is assumed that all the diodes are ideal with turn-on voltage V_t. The amount of charge seen by the reservoir will be referred as Q_{eq} which is equal to the charge on one of the capacitors when the capacitors are in serial connection and to the summation of charges on both capacitors when the capacitors are in parallel connection. Voltage on each capacitor is $(V - V_t)/2$ when the capacitors are in series connection and voltage on each capacitor is $V + V_t$ when the capacitors are in parallel connection.

We use the assumption that the movable capacitor plate is in sinusoidal motion. In Fig. 2.5, (a) is the plot of C (capacitance of each of the variable capacitors) vs. time, (b) is the plot of voltage seen on each of the parallelization switches (D_1, D_3); (c) is the plot of voltage seen on the serialization switch (D_2) and (d) is the plot of voltage seen on each of the variable capacitors vs. time.

At $t = 0$, $C = C_{max}$ the capacitance value stops increasing and is going to decrease for the subsequent duration of $T/2$. This causes the potential on the capacitors to rise. The potential difference between the terminals of diode 2 becomes negative and it stops conducting, and hence the capacitors (which were serially connected) stop receiving charge from the reservoir. The diodes 1 and 3 do not conduct either, until the voltage on each of the capacitors reach $V + V_t$, which were $(V - V_t)/2$ during serial connection. When the voltage on the capacitors reaches $V + V_t$, and C drops to $C_{max}(V - V_t)/(2(V + V_t))$ (point 1 of Fig. 2.6), the diodes 1 and 3 start conducting to constitute a parallel

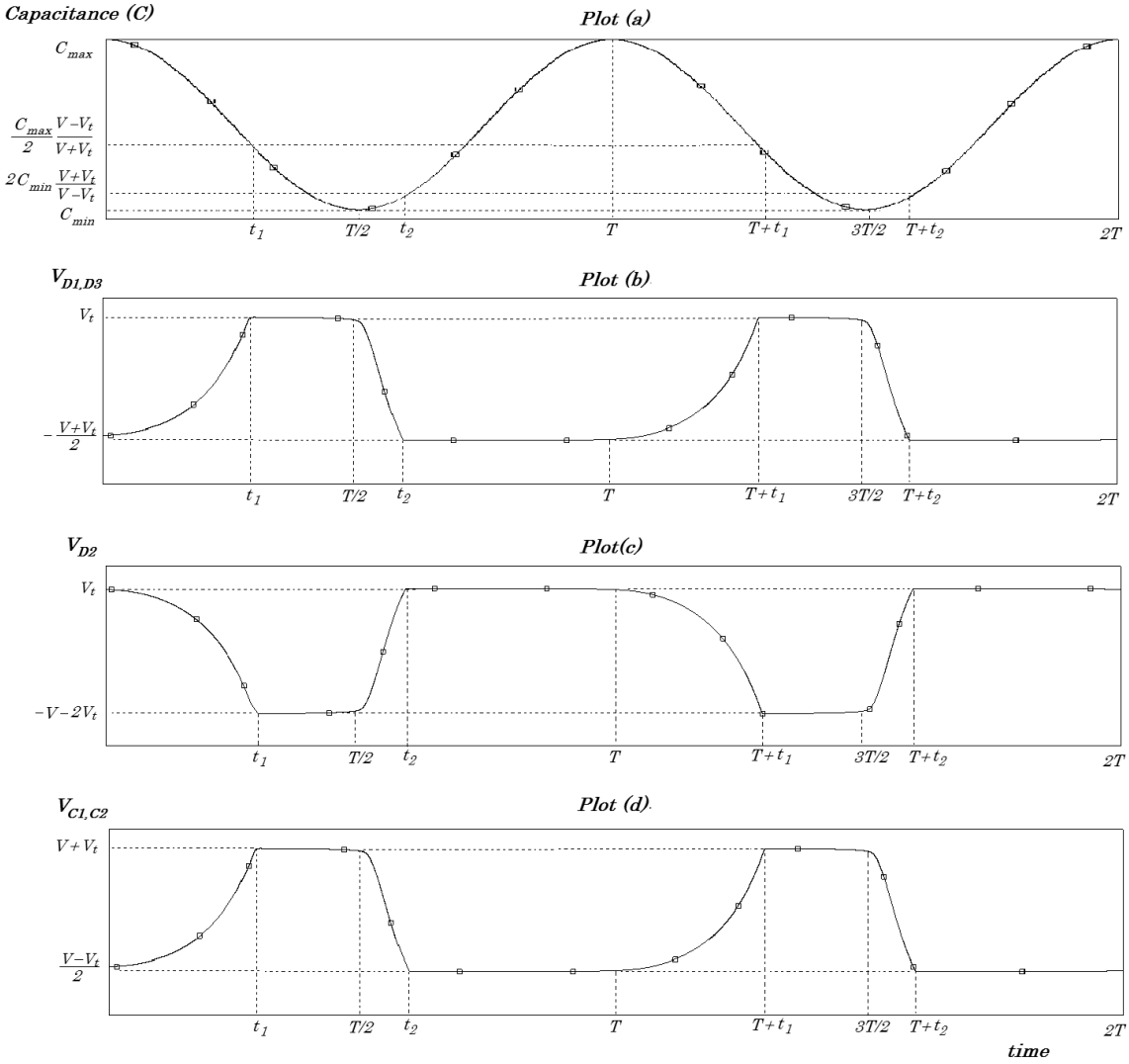

Figure 2.5: Time plots of the capacitance value (a), voltage on parallelization diodes D1 and D3 (b), voltage on serialization diode D2 (c), and voltage on capacitors C1 and C2 (d).

connected circuit, the current starts flowing towards the battery and the charge is accumulated on the battery while the capacitor potentials are kept at $V + V_t$. This charge transfer continues until C stops decreasing (point 2 of Fig. 2.6).

At $t = T/2$, $C = C_{min}$, C starts increasing. This means the potential on the capacitors will tend to decrease, they will go below $V + V_t$. Due to this potential drop the potential difference across the terminals of diodes 1 and 3 becomes negative and they stop conducting. Until the sum of the potentials of the capacitors become less than $V - V_t$, none of the diodes conducts. When

the potential on one of the capacitors is $(V - V_t)/2$, which happens when $C = 2C_{min}(V + V_t)/(V - V_t)$ (point 3 of Fig. 2.6), diode 2 conducts making the serial path active and the capacitors receive charge from the battery until C reaches C_{max} again (point 4 of Fig. 2.6).

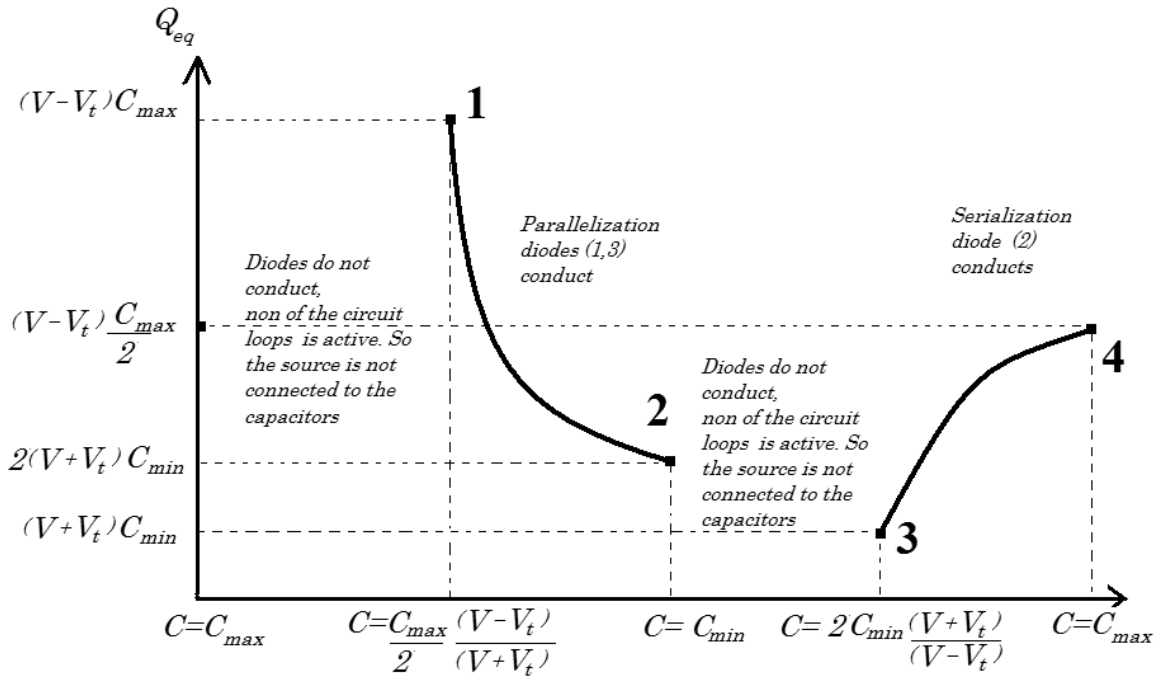

Figure 2.6: Plot of "Q_{eq}" versus C for one period.

We can make use of the Q_eq plot in Fig. 2.6 to calculate the charge transferred to battery in every step:

1 to 2:

$$C_{max}(V - V_t) - \frac{2C_{max}(V + V_t)}{\gamma} = C_{max}V(\frac{\gamma - 2}{\gamma}) - C_{max}V_t(\frac{\gamma + 2}{\gamma}) \qquad (2.2)$$

$$where \;\; \gamma = \frac{C_{max}}{C_{min}}$$

3 to 4: as "Q_{eq}" halves when serialized

$$\begin{aligned} \frac{C_{max}(V+V_t)}{\gamma} - \frac{C_{max}(V-V_t)}{2} = & \quad C_{max}V(\frac{2-\gamma}{2\gamma}) \\ & + \quad C_{max}V_t(\frac{\gamma+2}{2\gamma}) \end{aligned} \tag{2.3}$$

Summing up all charges:

$$\begin{aligned} Q_{net/cycle} &= C_{max}V(\frac{\gamma-2}{\gamma}) + C_{max}V(\frac{2-\gamma}{2\gamma}) \\ &\quad -C_{max}V_t(\frac{\gamma+2}{\gamma}) + C_{max}V_t(\frac{\gamma+2}{2\gamma}) \\ &= C_{max}V(\frac{\gamma-2}{2\gamma}) - C_{max}V_t(\frac{\gamma+2}{2\gamma}) \end{aligned} \tag{2.4}$$

The effect of γ on charge gain efficiency (on the net amount of stored charge) is given in Fig. 2.7. $Q_{net/cycle}/(0.5\ C_{max}\ V)$ is plotted versus different γ values. Here V_t is assumed to be equal to $V/10$. According to this plot, γ should be larger than 2 for the system to harvest energy. Increasing input mechanical energy will increase γ, and in turn stored energy; but beyond some point, increasing γ (mechanical energy) will not make a significant change in charge gain. So, in order not to waste input mechanical energy, we should set $C_max\ V$ factor (and so the electrostatic force) to an optimum level to keep γ around 30. Regarding the physical constraints, such as fraction limits, 30 is a reasonable value for a variable capacitor. Actually $\gamma = 100$ is already achieved in [9].

As long as γ is large, we can approximately write this equation as:

$$Q_{net/cycle} = \frac{1}{2}C_{max}(V - V_t) \tag{2.5}$$

Hence energy gain is,

$$E_{net/cycle} = \frac{1}{2}C_{max}\ V^2\ -\ \frac{1}{2}C_{max}\ V\ V_t \tag{2.6}$$

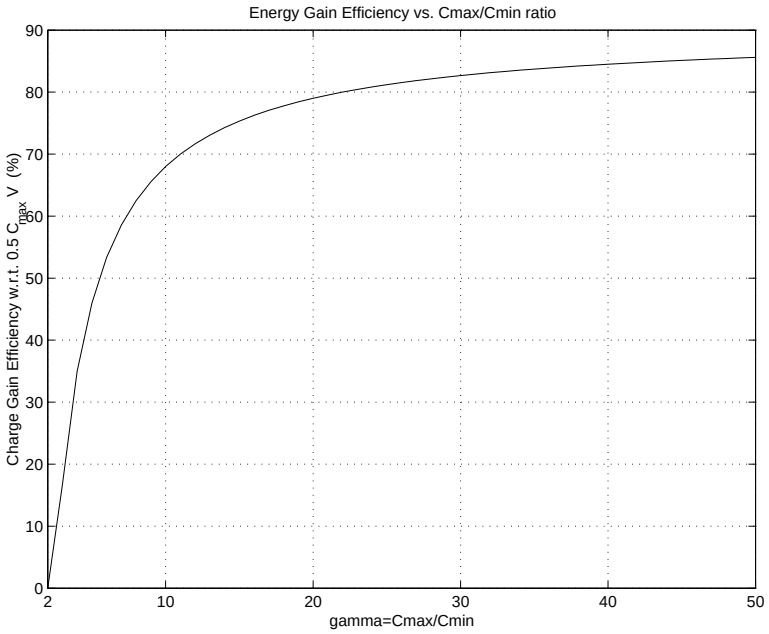

Figure 2.7: Plot of $Q_{net/cycle}/(0.5\ C_{max}\ V)$ vs. γ, showing dependence of charge gain on γ.

2.3.1 Simulations

In order to confirm the theoretical calculations with simulations, the system is modelled in SPICE as shown in Fig. 2.8. Here, other than the voltage source, the diodes and the variable capacitor blocks; there exist an AC source ($V3$) and a measurement block containing two resistors, an amplifier and a voltage-controlled voltage source. The AC source simulates the sinusoidally varying capacitance value, and the measurement block is used to measure the amount of charge entering the voltage source.

The variable capacitors are modelled using controlled sources as in Fig. 2.9. Here E is a voltage-controlled voltage source, its output directly gives voltage difference between the nodes of the capacitor. This voltage is multiplied with the signal coming from the AC source which represents the varying capacitance value, and this is sent to a 1F capacitor. The current passing through this capacitor is derivative of the signal introduced and this current is applied between the nodes of the variable capacitor through a current-controlled current source, F. This

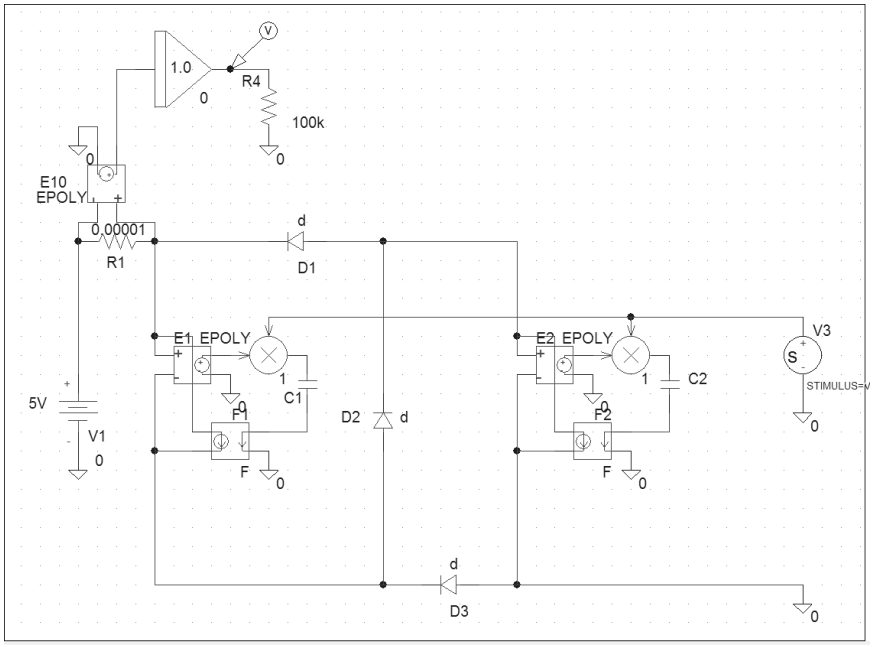

Figure 2.8: The P-Spice model of the variable capacitor-based circuit implementing the proposed energy conversion principle.

way, current passing through the variable capacitor is equal to $(d(C(t)*V(t)))/dt$, where $V(t)$ is the voltage difference between the nodes and $C(t)$ is the capacitance value at time t.

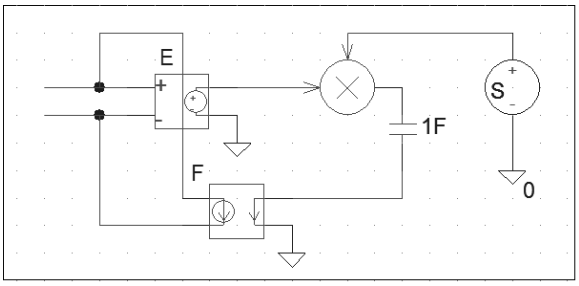

Figure 2.9: The P-Spice model of the variable capacitor.

Following is the SPICE simulation implemented using BAS416 diodes, ideal voltage source and ideal variable capacitors, i.e. without parasitic resistance. First a small time interval is presented to make the charge transfer behavior visible, then the linear increase in harvested energy is shown in long term:

a) For $V = 5$V, $V_t \simeq 0.4$V, $C_{max} = 1$nF, $\gamma = 20$, $f = 1$KHz Fig. 2.10 shows in a small time interval how the charge transfer occurs between the voltage

source and the rest of the circuit. Increase in value means charge is going from the capacitors to the voltage source, and decrease means charge is going out of the voltage source to the capacitors.

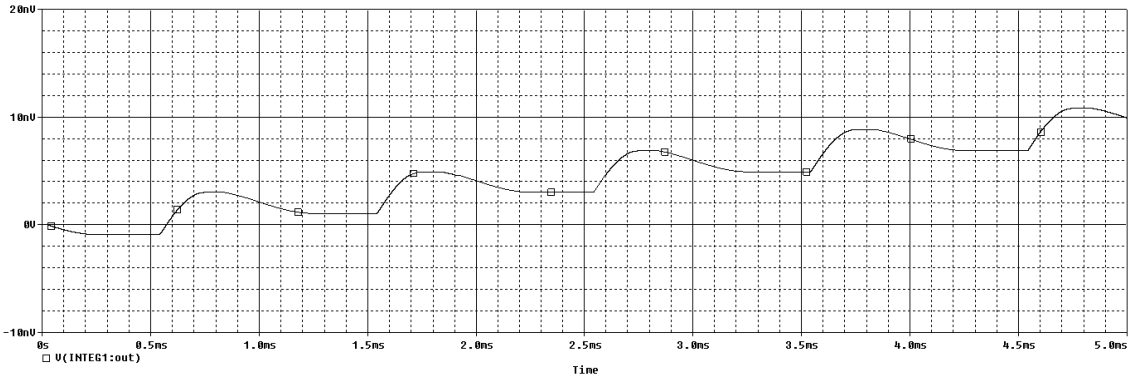

Figure 2.10: The plot of charge gain vs. time for a duration of 5ms when $V = 5$V, $V_t \simeq 0.4$V, $C_{max} = 1$nF, $\gamma = 20$, $f = 1$KHz showing the charge transfer behavior.

b) The "one second" plot of charge transfer for $V = 5$V, $V_t \simeq 0.4$V, $C_{max} = 1$nF, $\gamma = 20$, $f = 1$KHz is shown on Fig. 2.11. According to the theoretical calculations, we expect the charge gain at the end of 1 second to be 2.03μC and it turns out to be 2.0μC in the simulations. This 1.5% difference is due to the incomplete charge transfer and leakage currents. The energy harvested by this circuit in one second turns out to be 2μC * 5V=10 μJ.

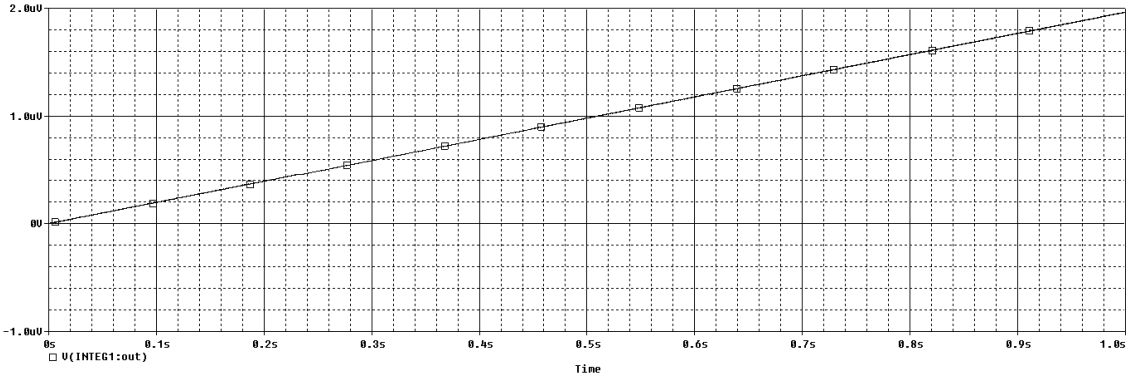

Figure 2.11: The plot of charge gain vs. time for a duration of 1s when $V = 5$V, $V_t \simeq 0.4$V, $C_{max} = 1$nF, $\gamma = 20$, $f = 1$KHz, showing the consistency of the theoretical calculations and simulations.

2.3.2 Experiment

An experiment is carried out using large variable capacitors and circuit elements as shown in Fig. 2.12. A DC power supply(the reservoir), two variable

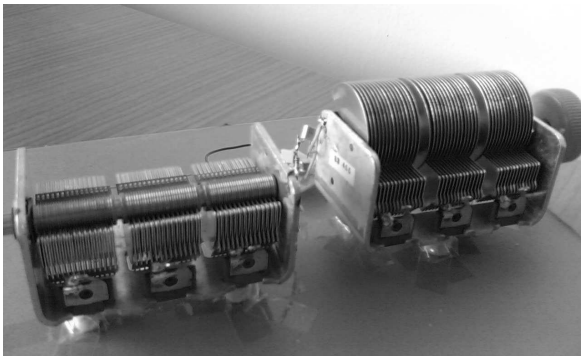

Figure 2.12: The macro level experiment setup employing two gang (variable) capacitors.

capacitors, and three diodes are used. The two variable gang capacitors (Ocean State Electronics-BC15500) are of value $45 - 1500$pF each. The diodes used are VISHAY-DPAD1 diodes, having $1pA$ reverse current and 1.5V turn-on voltage. To observe the current flow in the circuit a 1MΩ resistor - 68nF capacitor pair is connected in parallel with the 10MΩ oscilloscope probe and they are all connected in series to the reservoir. The diagram in Fig. 2.13 shows the experimental circuitry. The 68nF capacitor serves to increase the time constant so that the oscilloscope can track the current flow. The 1Mohm resistor is used to decrease the effect of noise coupling to the probe, but still there is significant amount of noise accompanying the data. In order to eliminate the noise, multiple measurements at zero source voltage are performed, and the averaged noise ($\sim$ 2nA) is subtracted from the current data.

The voltage read on the oscilloscope is equal to 10^7 times the current coming out of the voltage source. Fig. 2.14 gives a sample oscilloscope output for 6 seconds. When the experiment is carried out at $V = 40$V, $V_t = 1.5$V, $f = 1$Hz, $C_{max} = 1.5$nF, $C_{min} = 45$pF, Fig. 2.15, plot of charge entering the voltage source vs. time, is obtained. This plot is obtained in Matlab by integrating the current

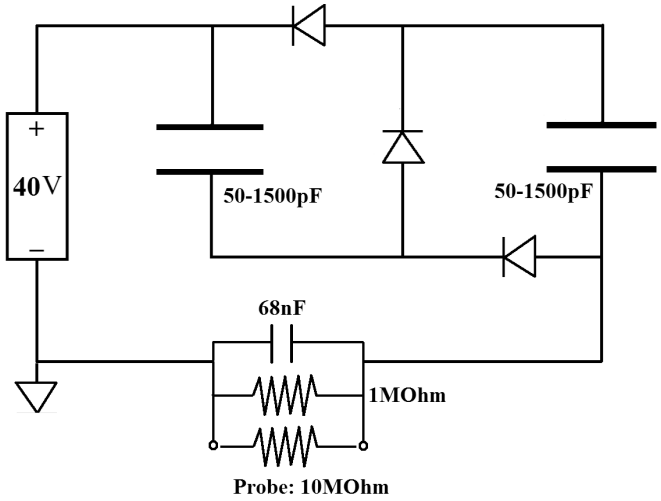

Figure 2.13: The circuit diagram of the experimental setup.

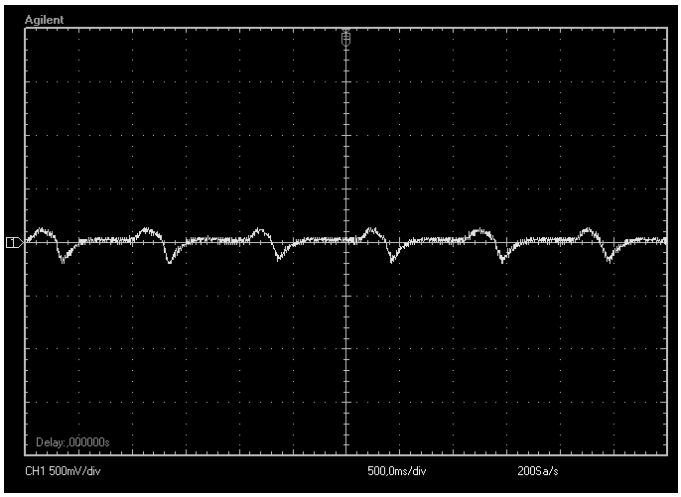

Figure 2.14: The sample oscilloscope image of current coming out of the voltage source.

measurement of oscilloscope. This current value is slightly higher than actual, as electrical fields existing in the environment and the experiment setup induce noise on the capacitors. When the noise is discarded, the amount of charge gained per second turns out to be 22nC. The theoretically expected value is 27nC in ideal case, but because of the charge leakage through the contamination between the plates of the capacitors, and the parasitic effects of the electrical components and measurement devices, the gain is 19% below the ideal case.

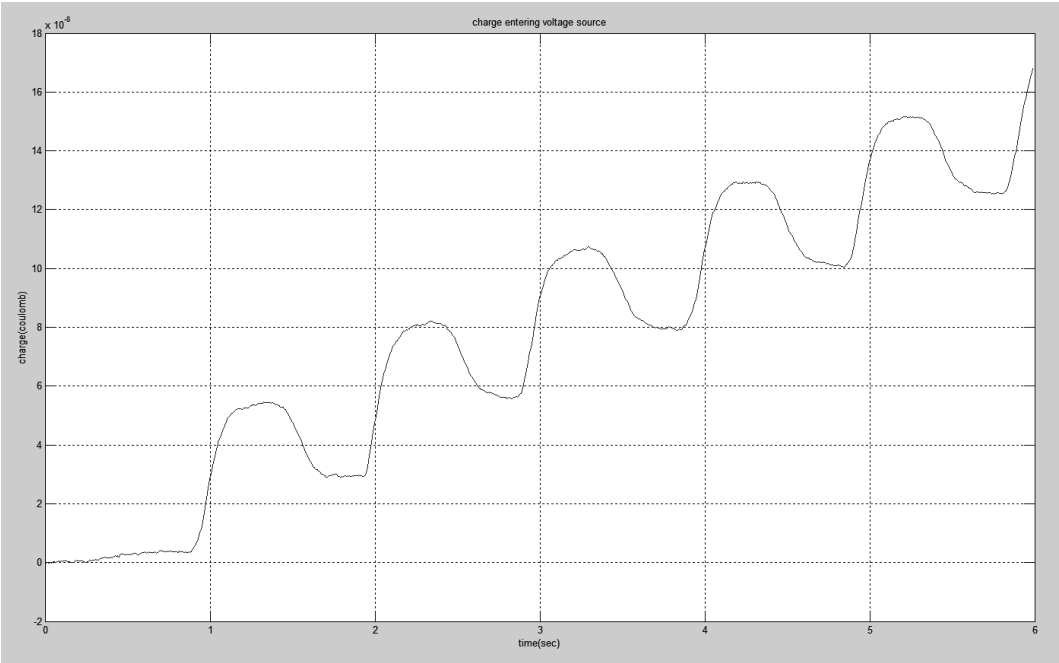

Figure 2.15: The plot of charge entering the voltage source, for the case $V = 40$V, $f = 1$Hz, $C_{max} = 1.5$nF, $C_{min} = 45$pF.

2.4 Self-Controlled Energy Converter Design Utilizing Capacitive Storage Element

A second circuit very similar to the one in Section 2.3 is shown in Fig. 2.16. There exist two capacitors and three diodes in this circuit as previously, but this time a capacitor substitutes for the reservoir. Voltage on the source capacitor is referred as V_s and voltage on each of the variable capacitors is referred as V_v.

This implementation is very similar to the previous one and the switching mechanism works the same way. D1 and D3 let the current flow from the variable capacitors to the source capacitor. As V_v becomes greater than $V_s + V_t$, D1 and D3 start conducting and all the capacitors are connected in parallel; and this

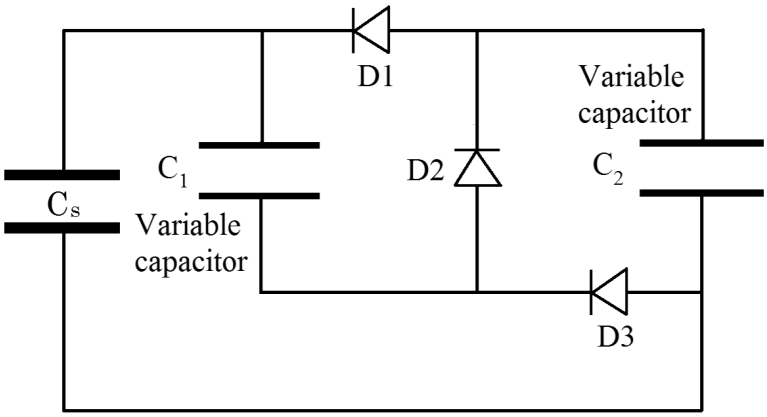

Figure 2.16: Self-controlled energy converter model utilizing diodes in place of switches and a capacitor in place of reservoir

can take place when C tends to decrease and force V_v to increase. D2 lets the current flow from the source capacitor to the variable capacitors. As V_v becomes smaller than $(V_s - V_t)/2$, it conducts connecting all the capacitors in serial. This can happen only when C value is increasing. When $V_s + V_t > V_v > (V_s - V_t)/2$ none of the diodes conduct and the charge residing on each of the plates remain the same.

Analysis of the circuit for one period of capacitor plate behavior (as given in Fig. 2.17) indicates that at $t = 0$ $V_v = q_v/C$ starts increasing, and D2 just stops conducting as V_s remains the same. q_v is fixed as there is no charge transfer until V_v reaches $V_s + V_t$ and D1 and D3 start conducting. As capacitors connect in parallel, charge is transferred to the source while C keeps decreasing. At $t = T/2$, C reaches C_{min} and the potentials of all the capacitors reach the highest level. C increases thereafter causing V_v to decrease. D1 and D3 do not conduct while V_v decreases. When V_v becomes $(V_s - V_t)/2$, D2 starts conducting and it conducts until $t = T$ and $C = C_{max}$ again, and the variable capacitors receive charge in that interval.

In this case, the source voltage is not fixed and it goes up as the energy stored in the system increases. So, it is better to trace the amount of charge accumulated on the capacitors in each cycle. We simply need to calculate the

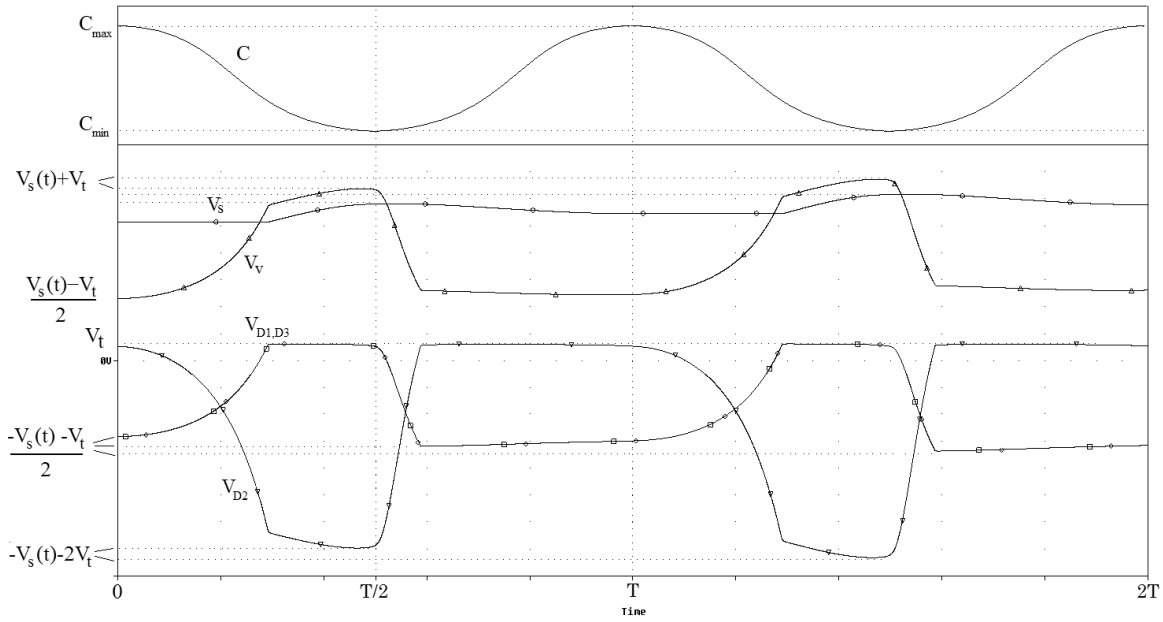

Figure 2.17: Time plots of the source voltage (V_s), capacitor voltage (V_v), and diode voltages (V_{D1}, V_{D2}, V_{D3}) vs. sinusoidal capacitor motion.

total amount of charge residing on the line connecting the source capacitor to the variable capacitors in order to determine the energy increase in the system.

The following is the charge analysis of one cycle: the total amount of charge (q_T) is calculated first when the capacitors are in serial connection, then when the capacitors switch to parallel connection and finally when the capacitors switch back to serial connection to calculate the increase in the total charge amount —and hence the total energy of the system.(See Fig. 2.18)

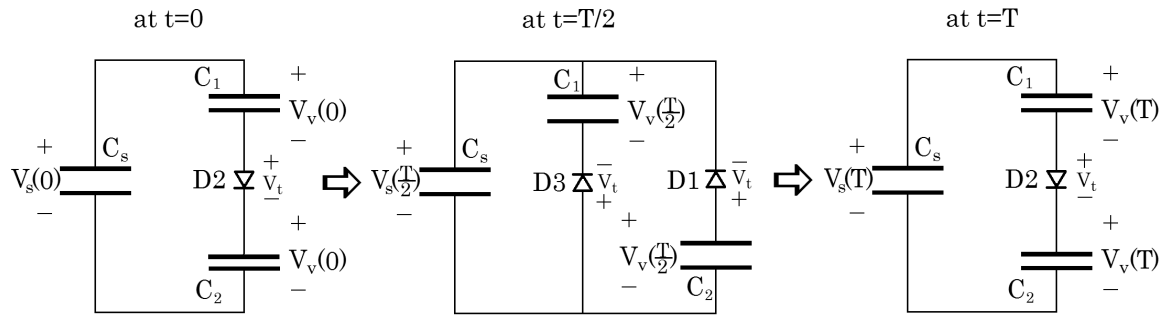

Figure 2.18: Circuit configurations at $t = 0$, $t = T/2$, $t = T$.

At $t = 0$,

$$\begin{aligned} q_T(0) &= q_s(0) + q_v(0) \\ &= V_s(0)C_s + V_v(0)C(0) = V_s(0)C_s + V_v(0)C_{max} \\ &= V_s(0)C_s + \frac{V_s(0) - V_t}{2}C_{max} \\ &= V_s(0)\frac{2C_s + C_{max}}{2} - V_t\frac{C_{max}}{2} \\ &= \frac{q_s(0)}{C_s}\frac{2C_s + C_{max}}{2} - V_t\frac{C_{max}}{2} \end{aligned} \tag{2.7}$$

$$q_s(0) = (q_T(0) + V_t\frac{C_{max}}{2})\frac{2C_s}{2C_s + C_{max}} \tag{2.8}$$

as, in serial connection,

$$\begin{aligned} V_s(0) &= 2V_v(0) + V_t \\ C(0) &= C_{max} \end{aligned}$$

At $t = \frac{T}{2}$,

$$\begin{aligned} q_T(\frac{T}{2}) &= q_s(0) + 2q_v(0) = 2q_T(0) - q_s(0) \\ &= 2q_s(0)\frac{2C_s + C_{max}}{2C_s} - V_tC_{max} - q_s(0) \\ &= q_s(0)\frac{(C_s + C_{max})}{C_s} - V_tC_{max} \end{aligned} \tag{2.9}$$

$$\begin{aligned} q_T(\frac{T}{2}) &= q_s(\frac{T}{2}) + 2q_v(\frac{T}{2}) \\ &= V_s(\frac{T}{2})C_s + 2V_v(\frac{T}{2})C(\frac{T}{2}) \\ &= V_s(\frac{T}{2})(C_s + 2C_{min}) + 2V_tC_{min} \end{aligned} \tag{2.10}$$

$$\Rightarrow q_s(\frac{T}{2}) = \left(q_T(\frac{T}{2}) - 2V_tC_{min}\right)\frac{C_s}{C_s + 2C_{min}} \tag{2.11}$$

as, in parallel connection,

$$\begin{aligned} V_s(\frac{T}{2}) &= V_v(\frac{T}{2}) - V_t \\ C(\frac{T}{2}) &= C_{min} \end{aligned}$$

At $t = T$,

$$\begin{aligned} q_T(T) &= q_s(\frac{T}{2}) + q_v(\frac{T}{2}) = \frac{1}{2}q_T(\frac{T}{2}) + \frac{1}{2}q_s(\frac{T}{2}) \\ &= \left(q_s(0)\frac{(C_s + C_{max})}{C_s} - V_t C_{max}\right)\frac{C_s + C_{min}}{C_s + 2C_{min}} - \frac{V_t C_{min} C_s}{C_s + 2C_{min}} \\ &= q_s(0)\frac{(C_s + C_{max})(C_s + C_{min})}{C_s(C_s + 2C_{min})} \\ &\quad -V_t\frac{C_s C_{max} + C_s C_{min} + C_{max} C_{min}}{C_s + 2C_{min}} \end{aligned} \tag{2.12}$$

$$\begin{aligned} q_s(T) &= (q_T(T) + V_t C(T))\frac{2C_s}{2C_s + C(T)} \\ &= q_s(0)\frac{(C_s + C_{max})(C_s + C_{min})}{(C_s + \frac{C_{max}}{2})(C_s + 2C_{min})} \\ &\quad -V_t\frac{C_s^2(C_{max} + 2C_{min})}{(C_s + 2C_{min})(2C_s + C_{max})} \end{aligned} \tag{2.13}$$

as, in serial connection,

$$\begin{aligned} V_s(T) &= 2V_v(T) + V_t \\ C(T) &= C_{max} \end{aligned}$$

Iteratively calculating the amount of charge stored at the end of n cycles;

$$\begin{aligned} q_s(nT) &= q_s((n-1)T)\frac{(C_s + C_{max})(C_s + C_{min})}{(C_s + \frac{C_{max}}{2})(C_s + 2C_{min})} \\ &\quad -V_t\frac{C_s^2(C_{max} + 2C_{min})}{(C_s + 2C_{min})(2C_s + C_{max})} \end{aligned} \tag{2.14}$$

$$\begin{aligned} q_s(nT) &= k^n q_s(0) \\ &\quad -(k^{n-1} + k^{n-2} + \cdots + k^0)V_t\frac{C_s^2(C_{max} + 2C_{min})}{(C_s + 2C_{min})(2C_s + C_{max})} \\ &= k^n q_s(0) - \frac{k^n - 1}{k - 1}V_t\frac{C_s^2(C_{max} + 2C_{min})}{(C_s + 2C_{min})(2C_s + C_{max})} \end{aligned} \tag{2.15}$$

$$where \quad k = \frac{(C_s + C_{max})(C_s + C_{min})}{(C_s + \frac{C_{max}}{2})(C_s + 2C_{min})}$$

and,

$$E_s(nT) = \frac{q_s(nT)^2}{2C_s} \tag{2.16}$$

As the charge stored in each cycle is not fixed but increases with increasing stored energy, the system voltage increases exponentially. One should make sure that the voltage limits of the load components are not exceeded. Fortunately, our implementation example is self limiting. The diodes used in place of switches control the voltage increase by the breakdown mechanism, they do not let the potential on them become greater than the breakdown level. A diode starts conducting (i.e. breakdown occurs) when the potential on it reaches a highly negative value. As $V_{D2} = -V_s - 2V_t$, D2 starts to conduct whenever $V_s + 2V_t$ reaches the breakdown voltage of the diode.(see figure 2.19)(Breakdown first occurs in D2 as the negative voltage on D1 and D3 equals $-\frac{V_s+V_t}{2}$.) So the V_s (and V_v) cannot exceed the breakdown level of the diode, and with a proper diode design the upper level of voltage can be specified by the designer.

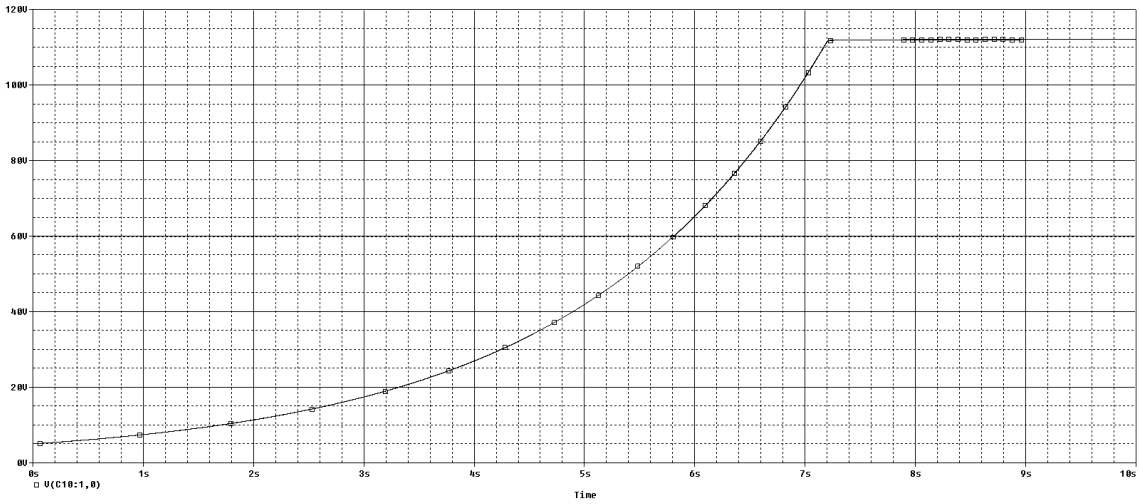

Figure 2.19: Plot of voltage on source capacitor vs. time. Its exponential increase stops at the breakdown level of diodes.

2.4.1 Simulations

The circuit in figure 2.20 is the modified circuit of section 2.3.1. Here the voltage source is replaced with a $1\mu F$ capacitor.

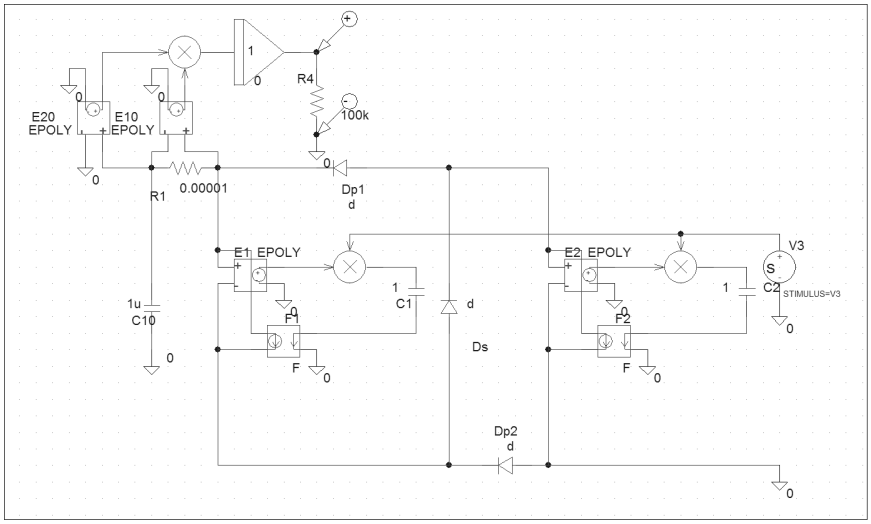

Figure 2.20: The P-Spice model of the circuit employing capacitor as the source.

Following is the SPICE simulation implemented using BAS416 diodes, ideal source capacitor and ideal variable capacitors, i.e. without parasitic resistance. First a small time interval is presented to make the charge transfer behavior visible, then the exponential increase in harvested energy is shown in long term:

a) For $C_s = 1\mu$F, $V_s(0) = 5$V, $V_t \simeq 0.4$V, $C_{max} = 1$nF, $\gamma = 20$, $f = 1$KHz figure 2.21 shows in a small time interval how the energy enters the source. Increase in value means charge is going from the variable capacitors to the source capacitor, and decrease means charge is going out of the source capacitor to the variable capacitors.

b) The "two second" plot of energy transfer for $C_s = 1\mu$F, $V_s(0) = 5$V, $V_t \simeq 0.4$V, $C_{max} = 1$nF, $\gamma = 20$, $f = 1$KHz is shown on figure 2.22. The energy converted by the system increases exponentially. At the end of one second 15.4μJ energy is stored and in the next one second 36.5μJ energy is stored. According to the theoretical calculations, we expect the stored energy at

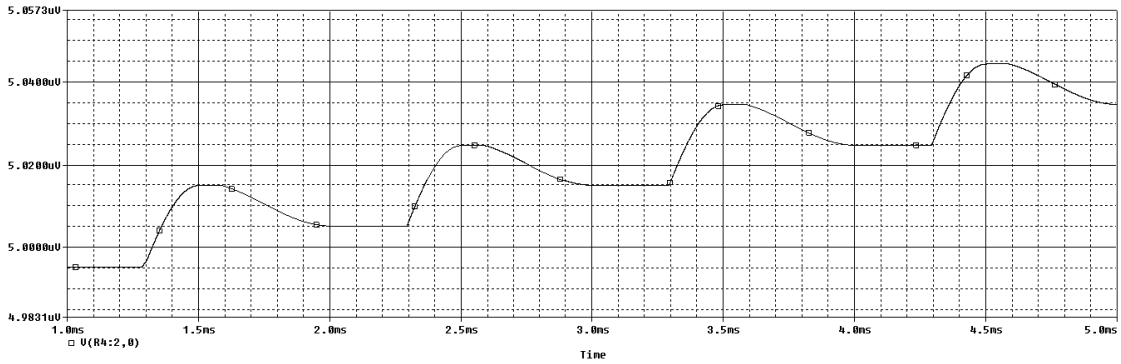

Figure 2.21: The plot of energy gain vs. time for a duration of 4ms when $C_s = 1\mu$F, $V_s(0) = 5$V, $V_t \simeq 0.4$V, $C_{max} = 1$nF, $\gamma = 20$, $f = 1$KHz showing the energy transfer behavior.

the end of two seconds to be 67.0μJ and it turns out to be 51.9μJ in the simulations. This time the error ratio is 22.5% and this is because as the voltage goes higher, the leakage through the circuit increases.

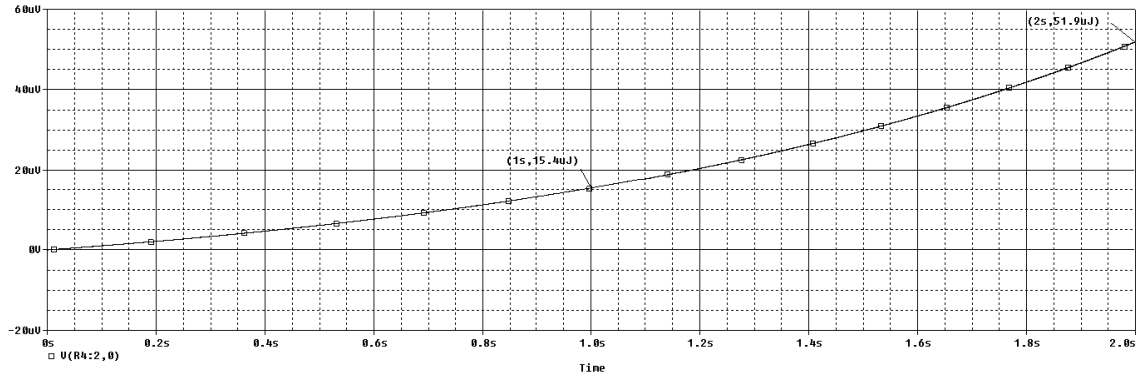

Figure 2.22: The plot of energy gain vs. time for a duration of 2s when $C_s = 1\mu$F, $V_s(0) = 5$V, $V_t \simeq 0.4$V, $C_{max} = 1$nF, $\gamma = 20$, $f = 1$KHz, showing the consistency of the theoretical calculations and simulations.

2.5 Discussions

The work presented throughout this chapter introduced and proved the functionality of an electrostatic mechanical to electrical energy converter design which differs from previous mechanical to electrical energy converters ([6–9]) with its simplicity, self controlling and ability to store the harvested power to the same

source it receives its initial electrical energy from. This system does not require an inductor or any active components to transfer energy to the source; and also there is no need for control-feedback circuitry as the switching is carried out by diodes rather than externally controlled switches.

An experiment is carried out at 81% efficiency. This efficiency loss originates from high leakage and parasitic effects. Diodes, variable capacitors, connections and the measurement setup are not perfectly suitable for energy storage. Especially the leakage through the components should be much less than the stored charge in one second in order to obtain high efficiency. When produced at the micro scale with specific diode and capacitor designs caring for energy economy, leakage and parasitics of the system can be reduced significantly and better efficiency can be achieved.

In this system, the power consumption of a control circuitry and the efficiency loss due to mismatch in feedback timing is eliminated, and absence of inductor and secondary reservoir means increase in dimension which in turn means increase in power gain. Yet the power gain of this electrostatic system is intrinsically low when designed in small dimensions. In the following chapter a further improvement is presented that will help to increase power gain.

Chapter 3

CHARGE EMBEDDED CAPACITOR — INCREASING EFFICIENCY

3.1 Introduction

The capacitive energy converter presented in Chapter 2 captures the energy of a mechanical force opposing the electric field. So, the amount of mechanical energy converted into electrical energy is determined by the work done against the electric field inside the capacitor. In order not to waste input mechanical energy, the electric field should be made large enough; but as the dimension of the capacitor is limited, capacitance —so the electric field— has an upper limit and there is a trade-off between the capacitance value and mechanical parameters such as mass, and the mass travelling distance. Given the dimensions, there is an optimum capacitor design that gives the best possible matching of mechanical and electrical energy content and maximum energy conversion; but usually even at this best point, converted energy remains below available energy level. So,

regardless of the applied mechanical energy there is a limit on extractable power set by the dimensions for a given frequency.

We can relieve the strict dependence of energy gain on dimensions by accumulating larger amount of charge on the capacitor —without setting the applied voltage to unacceptable values— through placing an electret inside the capacitor and trapping charge on this electret. This trapped charge creates extra and permanent electric field inside the capacitor and mechanical energy works against this increased electric field and does greater work.

Such a capacitor is also used in [23], where the current induced by the trapped charge passes through a resistive load and the delivered energy is dynamically consumed.

3.2 Application

In Fig. 3.1, there exists an explanatory example of charge embedded capacitor which is composed of three parallel plates with equal area, A. Here $-Q$ is trapped in the middle plate .

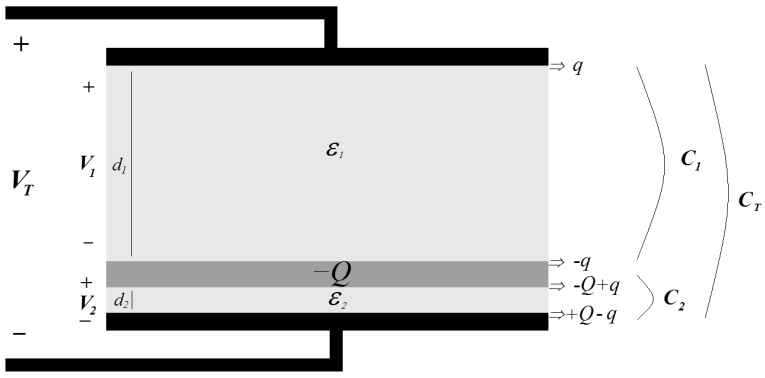

Figure 3.1: A charge embedded capacitor example. The capacitor is a parallel plate capacitor and there exists an electret in between the plates, and $-Q$ charge is trapped in this electret. The structure can be treated as two capacitors in series, first arising between the top plate and the electret, and second between the electret and the bottom plate.

We can treat this structure as two capacitors connected in series; the upper capacitor having capacitance $C_1 = (\epsilon_1 A)/d_1$ and the lower capacitor having capacitance $C_2 = (\epsilon_2 A)/d_2$. The charge is distributed according to the rule that equal amount of charge exists on the two plates of the capacitor. If q is the amount of charge on the upper plate, on the upper side of the middle plate there will exist $-q$, and the remaining $-Q + q$ amount of charge will reside at the lower side of the middle plate attracting the same amount of charge $(-Q + q)$ on the bottom plate. Now, to calculate q, we need to simply write the potential difference between the upper and lower plates as the summation of potential difference between the upper and middle plate and the potential difference between the middle and lower plate. In this context;

$$\begin{aligned} V_T &= V_1 + V_2 \qquad (3.1) \\ &= \frac{qd_1}{\epsilon_1 A} + \frac{(-Q+q)d_2}{\epsilon_2 A} \\ &= \frac{q}{C_1} + \frac{-Q}{C_2} + \frac{q}{C_2} \\ &= \frac{q}{C_T} - \frac{Q}{C_2} \\ \rightarrow \quad V_T + \frac{Q}{C_2} &= \frac{q}{C_T} \\ q &= (V_T + V_Q) * C_T \qquad (where\ V_Q = \frac{Q}{C_2}) \qquad (3.2) \end{aligned}$$

So, the capacitor acts as if the voltage applied between its plates is $V_T + V_Q$. This gives us the flexibility of raising the voltage and charge amount to a desired level without need for a high voltage supply, and also while doing this we will not be hindered by the upper voltage limit of the devices used together with the capacitor.

3.3 Using Embedded Capacitors Together with the Design Utilizing Voltage Source

In Fig. 3.2, the capacitors of the circuit analyzed in section 2.3 are replaced by charge embedded capacitors, and the following analysis calculates the amount of charge transferred to the battery per cycle.

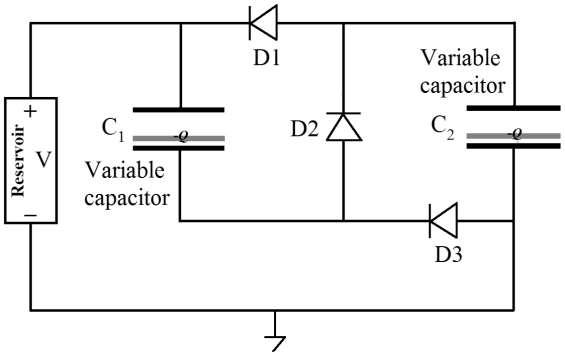

Figure 3.2: The model of the two capacitor, diode switched circuit employing charge embedded capacitors.

Here it is assumed that the capacitance varies sinusoidally, and the same cycle follows starting at $t = 0$ with $C = C_{max}$. While C decreases in the following $T/2$ period, the capacitors first keep the same charge on them until the voltage on each rise up to $V + V_t$. When the voltage level reaches the reservoir, the diodes 1 and 3 start conducting as the voltage of the capacitors tend to increase further. At that point (point 1 of Fig. 3.3), there exist $C_{max}((V - V_t)/2 + V_Q)$ amount of charge on each of the capacitors as they were serially connected just before $t = 0$, and the total amount of charge is $2C_{max}((V - V_t)/2 + V_Q)$ as the capacitors are now in parallel connection. Until $t = T/2$ and $C = C_{min}$ capacitors stay in parallel connection with voltage $V + V_t$ on them, delivering charge to the reservoir. When $C = C_{min}$ (point 2 of Fig. 3.3), charge amount on each of the capacitors is equal to $C_{min}(V + V_t + V_Q)$ and the total amount of charge is two times this value.

At $t = T/2$, $C = C_{min}$, C starts increasing causing the potential on the capacitors to decrease. So the charge transfer stops at that point, the capacitors can neither deliver charge nor receive, as voltage on each is lower than $V+V_t$ and higher than $(V - V_t)/2$. When sum of the potentials of the capacitors become $V-V_t$ (point 3 of Fig. 3.3), diode 2 starts conducting and connects the capacitors serially. At that moment, the charge seen by the reservoir is equal to the amount of charge residing on one of the capacitors and that is equal to $C_{min}(V+V_t+V_Q)$ as left from the previous period. After that the capacitors receive charge from the reservoir until $C = C_{max}$ and the charge on each of the capacitors reaches $C_{max}((V - V_t)/2 + V_Q)$ (point 2 of Fig. 3.3). One cycle is completed at that point.

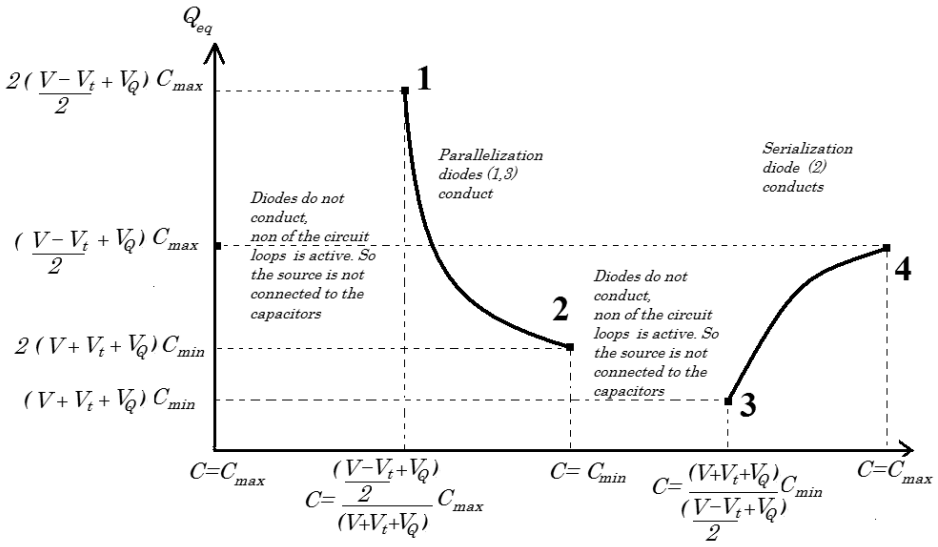

Figure 3.3: Plot of "Q_{eq}" versus C for one period when there exists an electret above the bottom plate. The electret has a potential difference of V_C with respect to the bottom electrode.

Calculating the charge transferred to battery in every step:

1 to 2:

$$\begin{aligned} & C_{max}(V - V_t + 2V_Q) - \frac{2C_{max}(V + V_t + V_Q)}{\gamma} \\ = \; & C_{max}V(\frac{\gamma - 2}{\gamma}) - C_{max}V_t(\frac{\gamma + 2}{\gamma}) + C_{max}V_Q(\frac{2\gamma - 2}{\gamma}) \end{aligned} \tag{3.3}$$

3 to 4: as "Q_{eq}" halves when serialized

$$\begin{aligned} & \frac{C_{max}(V + V_t + V_Q)}{\gamma} - C_{max}(\frac{V - V_t}{2} + V_Q) \\ = \; & C_{max}V(\frac{2 - \gamma}{2\gamma}) + C_{max}V_t(\frac{\gamma + 2}{2\gamma}) + C_{max}V_Q(\frac{1 - \gamma}{\gamma}) \end{aligned} \tag{3.4}$$

Summing up all charges:

$$\begin{aligned} Q_{net/cycle} &= C_{max}V(\frac{\gamma - 2}{\gamma}) - C_{max}V_t(\frac{\gamma + 2}{\gamma}) + C_{max}V_Q(\frac{2\gamma - 2}{\gamma}) \\ &+ C_{max}V(\frac{2 - \gamma}{2\gamma}) + C_{max}V_t(\frac{\gamma + 2}{2\gamma}) + C_{max}V_Q(\frac{1 - \gamma}{\gamma}) \\ &= C_{max}V(\frac{\gamma - 2}{2\gamma}) - C_{max}V_t\frac{\gamma + 2}{2\gamma} + C_{max}V_Q(\frac{\gamma - 1}{\gamma}) \end{aligned} \tag{3.5}$$

As long as γ is large, we can approximately write this equation as:

$$\begin{aligned} Q_{net/cycle} &= 0.5C_{max}(V - V_t) + C_{max}V_Q \\ &= 0.5C_{max}(V - V_t) + Q \qquad (where\ Q = C_{max}V_Q) \end{aligned} \tag{3.6}$$

This equation tells us that the amount of charge delivered to the reservoir is increased by Q, which is the amount of charge trapped in the capacitor. This improves the gain in proportion with the quantity of Q. If we are able to force high amount of charge (much larger than $0.5C_{max}V$) into the electret, then limitations on C_{max} become unimportant and we only need to maximize Q, regarding the mechanical energy input.

3.3.1 Simulations

The model in Fig. 3.4 is the modified PSpice model of our variable capacitor including the electret effect. A DC voltage source which stands for V_Q is added, as the capacitor equation is $q = C(V + V_Q)$ now.

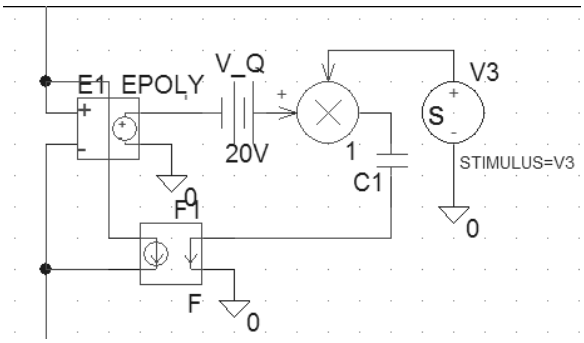

Figure 3.4: The P-Spice model of the variable capacitor with electret between the plates.

Replacing the old variable capacitor models with the new one, in PSpice model of our energy generating circuit, we obtained the output in Fig. 3.5 for $V = 5\text{V}$, $V_Q = 20\text{V}$, $V_t \simeq 0.4\text{V}$, $C_{max} = 1\text{nF}$, $\gamma = 20$, $f = 1\text{KHz}$. The

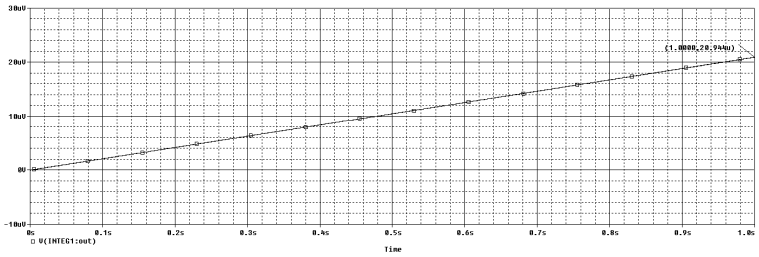

Figure 3.5: The plot of charge entering the reservoir vs. time for a duration of 1s when $V = 5\text{V}$, $V_Q = 20\text{V}$, $V_t \simeq 0.4\text{V}$, $C_{max} = 1\text{nF}$, $\gamma = 20$, $f = 1\text{KHz}$.

charge generated in one second is $20.9\mu\text{C}$ in the simulation. Theoretically, for a circuit without leakage current and employing ideal diodes it was expected to be $21.03\mu\text{C}$. Without the electret, this circuit would produce only $2.03\mu\text{C}$ charge in one second.

When we increase the capacitor number in the system, every new capacitor delivers approximately $\frac{\gamma-1}{\gamma}Q$ more charge to the reservoir in every cycle. The

simulation output in Fig. 3.6 verifies this situation. This simulation is done with $n = 5$ capacitors and $V = 5$V, $V_Q = 20$V, $V_t \simeq 0.4$V, $C_{max} = 1$nF, $\gamma = 20$, $f = 1$KHz. The expected charge gain per second is 79μC in ideal circuit case, and it is 76.7μC in the simulation.

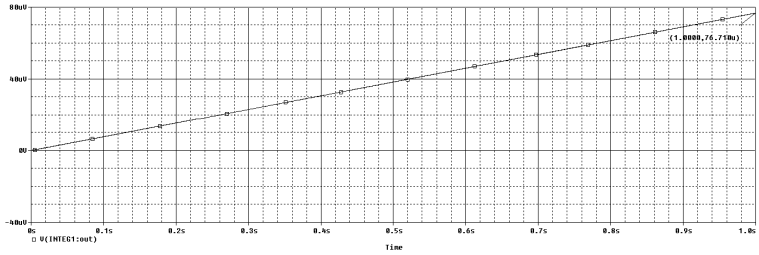

Figure 3.6: The plot of charge entering the reservoir vs. time for a duration of 1s when $V = 5$V, $V_Q = 20$V , $V_t \simeq 0.4$V, $C_{max} = 1$nF, $\gamma = 20$, $f = 1$KHz and 5 capacitors are employed in the system.

3.4 Using Embedded Capacitors Together with the Design Utilizing Capacitive Source

In this case the circuit in section 2.4 is implemented using charge embedded capacitors. (Fig. 3.7)

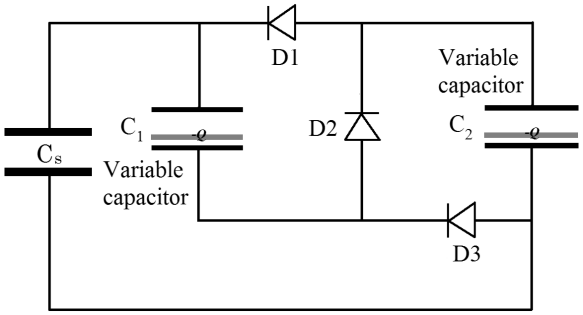

Figure 3.7: The model of the two charge embedded capacitor, diode switched circuit with source capacitor.

Here the same operation cycle is followed as in the former case in section 2.4 under the conditions that the capacitance varies sinusoidally and the diodes are ideal with turn-on voltage V_t.

Calculation of the increase in the amount of charge residing on the source capacitor at the end of one cycle:

At $t = 0$,

$$\begin{aligned} q_T(0) &= q_s(0) + q_v(0) \\ &= V_s(0)C_s + (V_v(0) + V_Q)C(0) \\ &= V_s(0)C_s + V_v(0)C_{max} + V_Q C_{max} \\ &= V_s(0)C_s + \frac{V_s(0) - V_t}{2}C_{max} + V_Q C_{max} \\ &= V_s(0)\frac{2C_s + C_{max}}{2} + V_Q C_{max} - V_t\frac{C_{max}}{2} \\ &= \frac{q_s(0)}{C_s}\frac{2C_s + C_{max}}{2} + V_Q C_{max} - V_t\frac{C_{max}}{2} \end{aligned} \tag{3.7}$$

$$q_s(0) = (q_T(0) - V_Q C_{max} + V_t\frac{C_{max}}{2})\frac{2C_s}{2C_s + C_{max}} \tag{3.8}$$

as, in serial connection,

$$\begin{aligned} V_s(0) &= 2V_v(0) + V_t \\ C(0) &= C_{max} \end{aligned}$$

At $t = \frac{T}{2}$,

$$
\begin{aligned}
q_T(\frac{T}{2}) &= q_s(0) + 2q_v(0) = 2q_T(0) - q_s(0) \qquad (3.9)\\
&= 2q_s(0)\frac{2C_s + C_{max}}{2C_s} + 2V_Q C_{max} - V_t C_{max} - q_s(0)\\
&= q_s(0)\frac{(C_s + C_{max})}{C_s} + 2V_Q C_{max} - V_t C_{max}
\end{aligned}
$$

$$
\begin{aligned}
q_T(\frac{T}{2}) &= q_s(\frac{T}{2}) + 2q_v(\frac{T}{2}) \qquad (3.10)\\
&= V_s(\frac{T}{2})C_s + 2V_v(\frac{T}{2})C(\frac{T}{2}) + 2V_Q C(\frac{T}{2})\\
&= V_s(\frac{T}{2})(C_s + 2C_{min}) + 2V_Q C_{min} + 2V_t C_{min}\\
\Rightarrow q_s(\frac{T}{2}) &= \left(q_T(\frac{T}{2}) - 2V_Q C_{min} - 2V_t C_{min}\right)\frac{C_s}{C_s + 2C_{min}} \qquad (3.11)
\end{aligned}
$$

as, in parallel connection,

$$
\begin{aligned}
V_s(\frac{T}{2}) &= V_v(\frac{T}{2}) - V_t\\
C(\frac{T}{2}) &= C_{min}
\end{aligned}
$$

At $t = T$,

$$
\begin{aligned}
q_T(T) &= q_s(\frac{T}{2}) + q_v(\frac{T}{2}) = \frac{1}{2}q_T(\frac{T}{2}) + \frac{1}{2}q_s(\frac{T}{2}) \\
&= \left(q_s(0)\frac{(C_s + C_{max})}{C_s} + 2V_Q C_{max} - V_t C_{max}\right)\frac{C_s + C_{min}}{C_s + 2C_{min}} \\
&\quad -\frac{V_Q C_{min} C_s}{C_s + 2C_{min}} - \frac{V_t C_{min} C_s}{C_s + 2C_{min}} \\
&= q_s(0)\frac{(C_s + C_{max})(C_s + C_{min})}{C_s(C_s + 2C_{min})} \\
&\quad +V_Q\frac{2C_s C_{max} + 2C_{max}C_{min} - C_s C_{min}}{C_s + 2C_{min}} \\
&\quad -V_t\frac{C_s C_{max} + C_s C_{min} + C_{max}C_{min}}{C_s + 2C_{min}}
\end{aligned}
\tag{3.12}
$$

$$
\begin{aligned}
q_s(T) &= (q_T(T) - V_Q C(T) + V_t C(T))\frac{2C_s}{2C_s + C(T)} \\
&= q_s(0)\frac{(C_s + C_{max})(C_s + C_{min})}{(C_s + \frac{C_{max}}{2})(C_s + 2C_{min})} \\
&\quad +V_Q\frac{2C_s^2(C_{max} - C_{min})}{(C_s + 2C_{min})(2C_s + C_{max})} \\
&\quad -V_t\frac{C_s^2(C_{max} + 2C_{min})}{(C_s + 2C_{min})(2C_s + C_{max})}
\end{aligned}
\tag{3.13}
$$

as, in serial connection,

$$
\begin{aligned}
V_s(T) &= 2V_v(T) + V_t \\
C(T) &= C_{max}
\end{aligned}
$$

So in each cycle,

$$
V_Q\frac{2C_s^2(C_{max} - C_{min})}{(C_s + 2C_{min})(2C_s + C_{max})} \approx V_Q C_{max} = Q \qquad for\ C_s \gg C_{max} \gg C_{min} \tag{3.14}
$$

amount of extra charge is stored to the system as in the previous implementation and the same conclusion is also valid for this case.

3.4.1 Simulations

The Spice simulation with two variable capacitors give the following output (Fig. 3.8) for $C_s = 10\text{nF}$, $q_s(0) = 150\text{nC}$, $V_Q = 20\text{V}$, $V_t \simeq 0.4\text{V}$, $C_{max} = 1\text{nF}$, $\gamma = 20$, $f = 1\text{KHz}$:

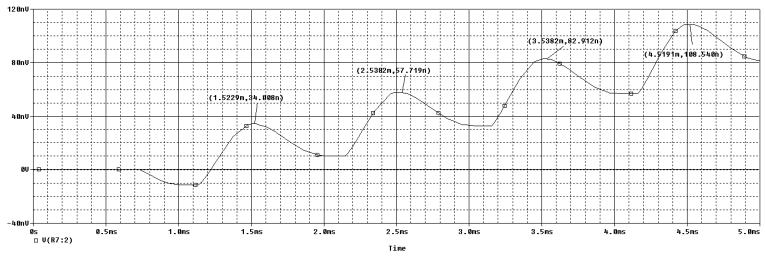

Figure 3.8: The plot of charge entering the reservoir vs. time for a duration of 5ms when $C_s = 10\text{nF}$, $q_s(0) = 150\text{nC}$, $V_Q = 20\text{V}$, $V_t \simeq 0.4\text{V}$, $C_{max} = 1\text{nF}$, $\gamma = 20$, $f = 1\text{KHz}$.

In the third cycle, charge increases from $q_s = 150 + 57.7\text{nC}$ to $q_s = 150 + 82.9\text{nC}$. So the gain is 25.2nC. Making use of the analytical calculations it is expected to be 26.5nC. Without the electret the expected gain is only 8.6nC in this cycle.

3.5 Discussions

The simulations show that this improvement may increase the gain by high percentage. Other than the load limitations, the physical constraints on electrical circuitry —such as limited area and small dielectric constant— no longer restrict us, and we are only restricted by the mechanical energy input.

One possible problem of this application is about the stability of embedded charge in long term. It may leak as time passes and need to be replenished. To partly overcome this problem, the best possible optimization for dimension, timing and charge amount of the trapping mechanism should be achieved in order

to meet the requirements of a specific application. One advantage is that even when the charge leaks out completely the system continues harvesting power obeying the working principle of the converter of Chapter 2.

This improvement can also be used in other applications employing capacitors, to increase efficiency. In any application where there is a limit on the source voltage but high charge accumulation is required; and for the reverse situation, when less charge accumulation is required although high voltage is applied on the capacitor, this trick can be used with proper choice of the polarization of the stored charge.

Chapter 4

MECHANICAL CONSIDERATIONS

4.1 Introduction

When designing a mechanical-to-electrical energy converter, electrical and mechanical circuits should be considered simultaneously. First of all, the variable capacitors should be effectively designed to exert high enough electrostatic field so that they are coupled to the mechanical system while meeting the electrical energy needs of the application. The mechanical energy capturing mechanism should be matched to the external source impedance and should store high enough amount of mechanical energy. On the other hand, given a limited volume and restrictions on physical parameters, all the electrical and mechanical parameters become strictly dependent on each other. So, the mechanical and electrical circuits should be designed and optimized simultaneously to reach maximum efficiency.

The converter can be implemented in various ways, and for every specific application, a different circuitry and operation scheme best captures the available

mechanical energy and converts with high efficiency. If the mechanical energy is provided from a source that can apply force directly on the converter, a mechanical interface (such as a membrane) moving under effect of this force captures and delivers the motion. Otherwise, when there is mechanical acceleration in the medium, the energy of this acceleration is captured through a mass suspended to the casing. Such converters, utilizing a mass showing inertia to the motion of the casing, are called inertial converters. As inertial conversion is suitable for a wider range of energy sources, we concentrate on such a design. Inertial converter designs, design concepts and constraints are discussed in the following sections.

4.2 Mechanical Circuit

An inertial electrostatic converter can be constituted in various ways depending on the choice of motion-affected parameter. Either area or distance or dielectric constant of the capacitor can be altered through the effect of the mass motion. The in-plane overlap type capacitor described in [5] is an example to the converters where the area of the capacitor is altered, and the distance between the plates is altered using the in-plane gap closing type capacitor and the out-of-plane gap closing type capacitor [5]. A converter in which the dielectric constant is altered through motion can be implemented using micro-fluidics technology.

Every design exhibits a different damping characteristic throughout one operation cycle, the electrical force between the plates of the capacitor may be constant or varying relative to the motion depending on the design. So, each of these designs will result in a different conversion efficiency when matched to the electrical circuitry. Depending on the volume restrictions, input energy characteristic, and physical constraints specific to the application, the mechanical

circuit giving highest conversion efficiency may change. In the following section, common factors that effect the power output and conversion efficiency and constraints on these factors are discussed.

4.2.1 Efficiency Analysis — Design Optimization

Given the available input mechanical power, an optimization is required for the mechanical and electrical circuitries to achieve optimum conversion efficiency. For a mass-spring system oscillating under effect of an externally applied motion, and altering the distance between the plates of the capacitor, the intrinsic parameters to consider are the power content of the external mechanical energy ($P(f)$), fluid damping resisting to the motion of mass (F_{fric}), and average electrical resistance serial to the capacitors (R_{av}); and the controllable parameters to optimize are frequency (f), mass weight (m), capacitor area (A), minimum distance between the plates of the capacitor (d_{min}), and voltage of the source (V).

We need to match the available, mechanically stored, electrically captured, and required power levels. Available power at the frequency of operation, the power captured and stored by the mass at that frequency, and power stored to the electrical source should be maximized to exceed the power requirement of the application.

Firstly, the power content of the frequency of operation should meet the power requirement:

$$P(f) \gg P_{req} \tag{4.1}$$

This usually implies operating at low frequencies where the power level is higher.

Secondly, the mechanically stored energy should be larger than the electrically captured energy. So the oscillating mass(m), the resonance frequency(f), and the maximum velocity of the mass (v_{max})(so the travelling distance,X) should

be set to highest possible values:

$$\frac{mv_{max}^2}{2} = 2\pi^2 m X^2 f^2 \gg QF\ E_{net/cycle} \tag{4.2}$$

QF is the quality factor of the mechanical system.

The time constant of the capacitors' charge-discharge process is a limiting factor for the power gain. The power gain linearly increases with increasing C_{max} (see equations 2.6, 2.16) and f; but $C_{max}f$ multiplier cannot be made arbitrarily large as the period of operation should be larger than the time constant:

$$\tau = \alpha R_{av} C_{max} \leq f^{-1} \tag{4.3}$$

α is the safety margin.

Applying this condition to Eq. 2.6 we get the following upper limit for power gain;

$$P_{net} = E_{net/cycle} \times f = 0.5(V - V_t)VC_{max}f \leq \frac{0.5(V - V_t)V}{\alpha R_{av}} \tag{4.4}$$

and this limit should be greater than the required power level:

$$\frac{0.5(V - V_t)V}{\alpha R_{av}} \gg P_{req} \tag{4.5}$$

This also means that there exists an optimal C_{max} value for every frequency, and when deciding on the resonance frequency the maximum achievable C_{max} value should be considered.

Lastly, the electrical stored power (see Eq. 4.6) is the parameter of interest which should not only exceed the required power level of the application but also increased further to the optimum level.

$$P_{net} = \frac{(V - V_t)V\epsilon A f}{d_{min}} \tag{4.6}$$

Direct observation tells that A, V and $1/d_{min}$ should be increased; but A is limited as the total volume is limited, d_{min} is restricted by the process, and V should remain within the breakdown limit. Also, there is actually a maximum P_{net} value that ensures matching between external energy source and the system.

At the dimension of our interest, i.e. at micron level, the most limiting part is the mechanical energy capturing mechanism rather than the electrical circuitry. For the electrical side, in a limited volume, the power output can be increased by increasing source voltage, or using high permittivity medium in between the capacitors (making use of microfluidics technology), or employing the charge embedded capacitors presented in Chapter 3. On the other hand, mechanical parameters (mass, spring constant and travelling distance) are strictly restricted within the given dimensions. So any improvement on increasing the mechanically stored power will significantly increase conversion efficiency. Actually one such idea, coulomb-force parametric generator (CFPG), is proposed by Mitcheson et al. in [4,26,28]. They offer not to use the mass at resonance, but rather increase the electrical force damping of the mass motion to such a level such that the mass moves only at the portion of the external motion cycle where the acceleration is maximum. So, lowering the quality factor of the mechanical circuit, the amount of power delivered to the electrical circuit is increased. Except the cases where it is compulsory to have a sinusoidal variation in capacitance for the feedback unit or an internal L-C resonance circuit to function, this operation principle can increase the conversion efficiency. It is applicable to our energy converter as there is no feedback unit or electrically resonating part requiring regular motion to function.

4.2.2 Simulations

Handling the constraints mentioned above separately lead to complexity, but unfortunately the system of interest has multiple nonlinearities, and there is no closed form power gain expression in terms of input mechanical power and system parameters. In order to observe the behavior of the system, it is simulated in PSpice using the analogy between mechanical and electrical components.

The mechanical model of the system is given in Fig. 4.1. It is an out-of-plane gap closing type converter. Although it is not the most efficient conversion mechanism, it is used in the simulations due to its simplicity. Attempts of simulating the in-plane gap closing comb drive system were not successful as higher order terms arose and the system complexity led to convergence problems.

This converter employs a simple parallel plate capacitor, the upper plate of which is movable. This plate constitutes a resonance system together with the springs it is attached to. The casing moves under effect of the external motion and its position is $x(t)$ with respect to ground, and the plate shows inertia to the motion of the casing that is transferred to it through the springs and it oscillates up and down, its position being $y(t)$ with respect to ground.

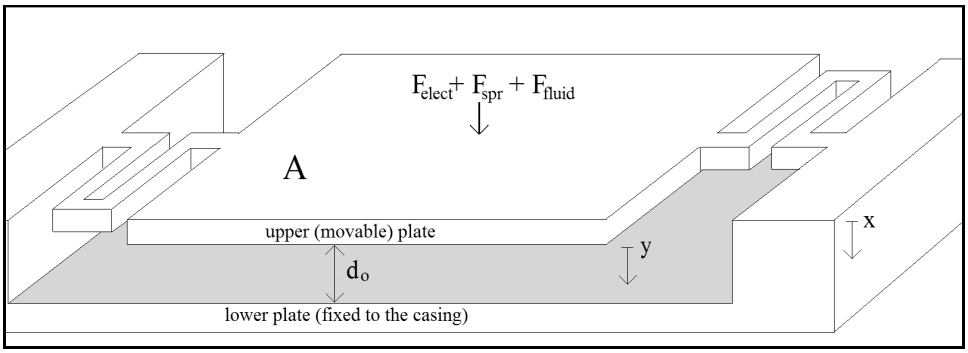

Figure 4.1: Model of out-of-plane gap closing type converter.

The mass (plate) in Fig. 4.1 experiences three main forces which altogether determine the acceleration of the mass. F_{elect} is the electrostatic force between the plates, F_{spr} is the force applied by the stretched spring and F_{fluid} is the force applied by the fluid (air) compressed between the plates:

$$\begin{aligned} m\ a(t) &= F_{elect} + F_{spr} + F_{fluid} \\ m\ \frac{d^2y(t)}{dt^2} &= \frac{\epsilon A V_c(t)^2}{d(t)^2} + k(x(t) - y(t)) + F_{fluid} \\ m\ \frac{dI_y(t)}{dt} &= \frac{\epsilon A V_c(t)^2}{d(t)^2} + k(\int I_x(t) - \int I_y(t)) + F_{fluid} \\ m\ \frac{dI_y(t)}{dt} &= \frac{\epsilon A V_c(t)^2}{2d(t)^2} + k(\int I_z(t)) + F_{fluid} \end{aligned} \tag{4.7}$$

where m is mass, $a(t)$ is acceleration of mass, $V_c(t)$ potential of each of the capacitors, ϵ is permittivity of the medium, A is the area of the plates and $d(t)$ is the distance between the plates of the capacitor, d_o is the initial value of $d(t)$(when spring is at zero energy position), k is the spring constant, and;

$$d(t) = d_o + x(t) - y(t)$$

$$z(t) = x(t) - y(t)$$

$$I_x(t) = \frac{dx(t)}{dt},\ I_y(t) = \frac{dy(t)}{dt},\ I_z(t) = \frac{dz(t)}{dt}$$

The corresponding circuit model of Eq. 4.7 is given in Fig. 4.2. F_{elect} is analogous to a voltage source, value of which depends on I_z, so it is actually a feedback controlled voltage source.

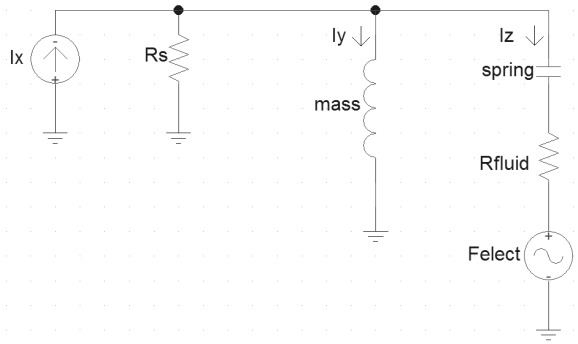

Figure 4.2: Electrical circuit analogy of the mass-spring system.

In the simulations a current-controlled current source is used to sense I_z and its integral is taken to find $z(t)$, then making use of mixers F_{elect} is calculated and fed to the mechanical circuit. $z(t)$ is also used to calculate the capacitance and the capacitance value is fed to the electrical circuit of Chapter 2; and the electrical circuit feeds $V_c(t)$ value to the mechanical part for F_{elect} calculation. There is also two other voltages added to F_{elect} representing the force applied by the wall used for stopping the upper plate before it hits the lower plate and preventing from traveling too high. Actually in the simulations the condition of hitting the wall is avoided due to two problems. When the plate hits the wall, other types of forces will appear which are not considered in the simulation, so

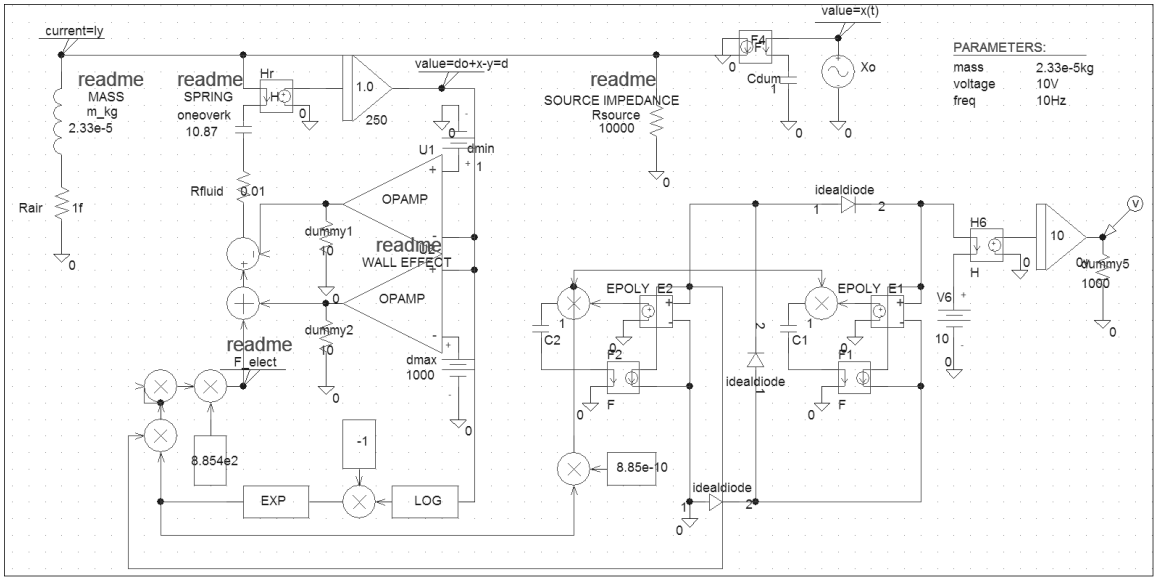

Figure 4.3: PSpice simulation of the overall system.

the simulation will not be all correct; and also most of the time wall collisions could not be solved by the simulator and the simulation ended giving an overflow error. So only smooth resonance case is analyzed throughout the simulations. Although we wished to observe the conversion efficiency of CFPG type operation, it is not analyzed either due to overflow errors.

Setting A to 1cm^2, f to 10Hz, m to 2.33×10^{-5}kg, X_o (amplitude of external motion) to 1mm, and choosing a high source impedance, the system is simulated for different V (source voltage) values. Optimum d_o value giving maximum power output for each voltage level is obtained. In the simulations, F_{fluid} is set to zero(assuming the system is in vacuum), otherwise the damping force is very high and it dominates the motion and there is no energy generation unless the external energy is extremely high. This is another important constraint that makes this generator useless.

The sample plots for plate motion (Fig.4.4) and energy transfer to the electrical source (Fig.4.5) are obtained for $V = 10$V and $d_o = 225\mu$m. This d_o value is the limit for hitting the wall and maximum power gain is obtained here. Plate oscillates smoothly as seen in Fig.4.4. C_{max} turns out to be 15pF and $\gamma = 6$;

and with these values expected power gain is 5nW which is very close to the simulation output.

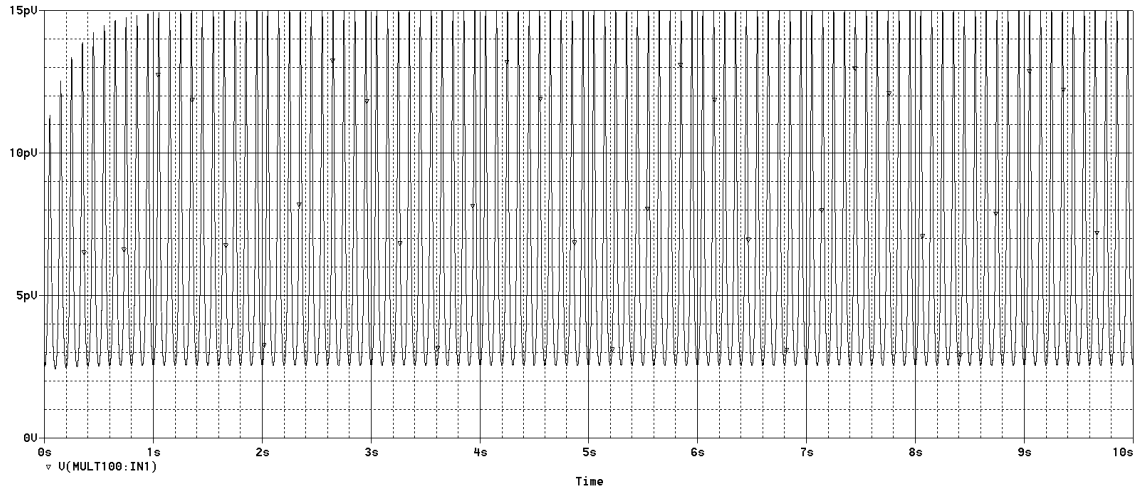

Figure 4.4: Distance between the plates of the capacitor vs. time.

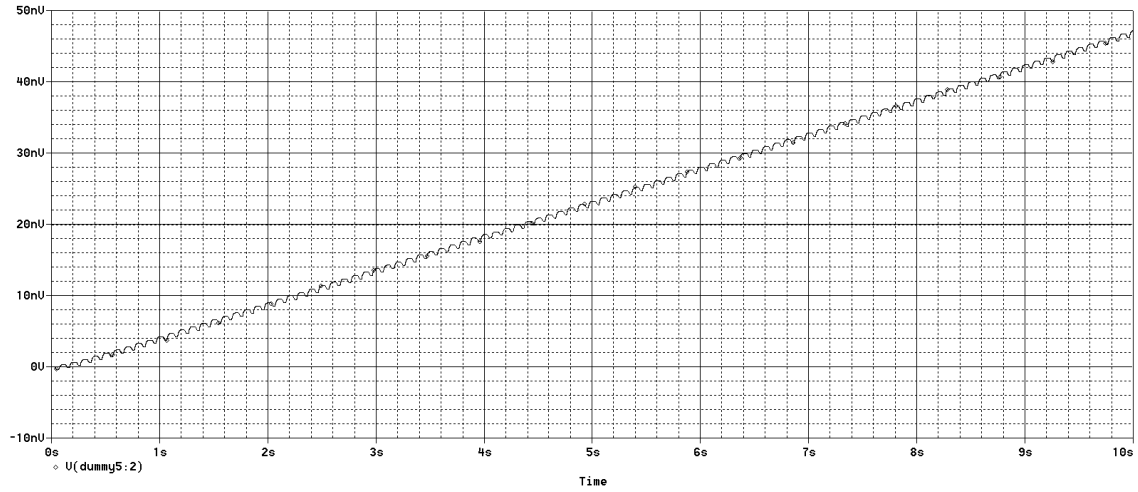

Figure 4.5: Energy transferred into the electrical source.

For increasing source voltages, the corresponding maximum power gain is plotted in Fig. 4.6. According to the plot the optimum voltage is around 28V and maximum power gain is $\sim$ 10nW.

This condition is expected, as the external source and mechanical system will be matched to each other for a specific load (electrical energy capturing). At optimum point, F_{elect} is neither too high to pull down and contract the travelling range of the plate, nor too low to capture only a small portion of the mechanical energy.

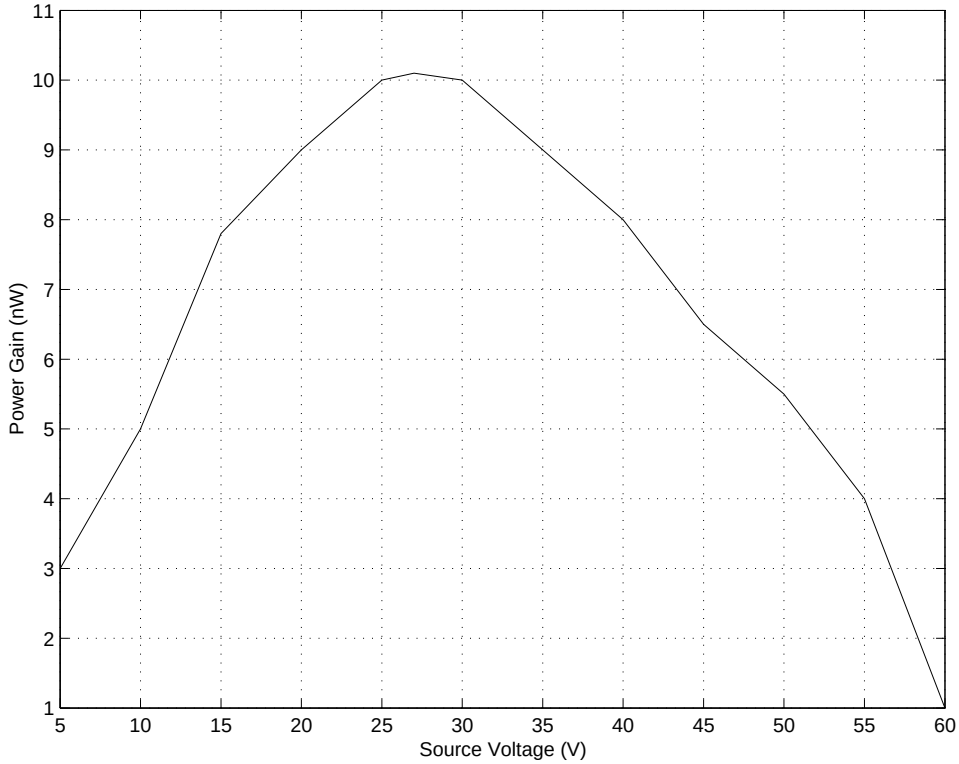

Figure 4.6: Power output vs. source voltage.

4.3 Discussions

The mechanical circuit of the generator can not be designed separately but rather it should be considered together with the electrical circuitry. After achieving the maximum mass (m) value in the given volume, spring constant, travelling distance of mass, initial distance between the plates should all be decided in coordination with the electrical parameters. The complete system should be optimized to match the source of external motion.

In mechanical sense, the energy converter design presented in this thesis is advantageous as it adapts to fluctuations in mechanical signal when the motion does not perfectly repeat itself at a constant frequency. This is the common issue of many electrostatic mechanical-to-electrical energy converters. The electrical circuits of Chapters 2 and 3 are actually self adaptive as they do not employ externally controlled switches and feedback circuitry. They do not need regular,

fixed frequency motion. Whenever the electrostatic force is dominated by the mechanical force, it generates charge to be stored in the reservoir. Otherwise no current flows through the diodes other than leakage and the capacitors are kept at a constant energy level.

As capacitors are commonly used in micro sensor-actuator applications, there exist various MEMS capacitor designs that are applicable to our system. Among those, the most suitable one is comb-drive which uses the volume most effectively through tightly placed plates in parallel as in Fig. 4.7. As the power gain increases proportionally with capacitance, these high capacitance structures are useful for our applications. One other alternative is the honeycomb model shown in Fig. 4.8 which uses the area effectively in vertical dimension.

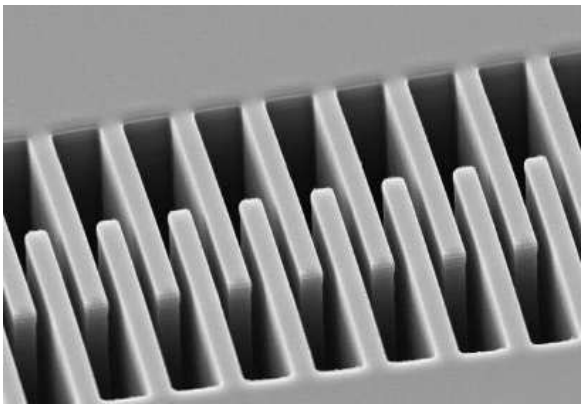

Figure 4.7: Comb capacitor

Our aim is to further improve the capacitor designs given above for our system. Making use of micro-fluidics technology, filling a high dielectric constant fluid in between the plates of a capacitor, it may be possible to get larger capacitance values. Also a variable capacitor with fixed plates but varying permittivity can be obtained by using two types of fluids with different dielectric constants and circulating them with the help of a pump working under effect of external mechanical energy.

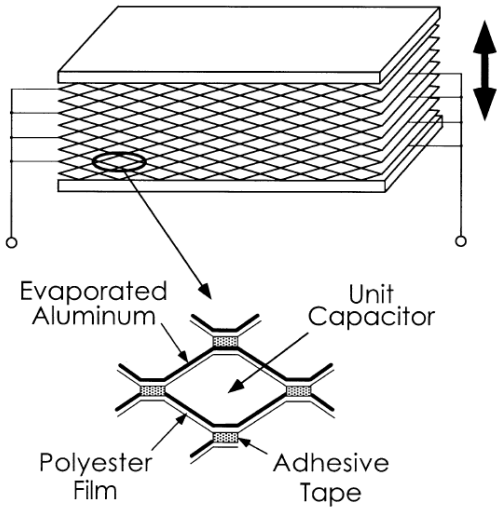

Figure 4.8: Honeycomb capacitor

Volume limitation is also crucial for mechanically stored energy and it restricts the power output of the generator seriously. In order to overcome this problem, a CFPG type generator [4] will also be designed and fabricated.

Chapter 5

CONCLUSION

This thesis introduced an electrostatic mechanical-to-electrical energy converter design which is MEMS compatible and free of magnetic effects. This converter employs only variable capacitors and switches, and it is capable of generating new charge. It makes use of serial-parallel switching to generate charge; capacitors are charged up in serial connection and discharged in parallel connection. This way a pure electrostatic charge generating device came up. Being purely electrostatic and pure silicon device, it is advantageous over other electrostatic converters utilizing inductors. One other advantage is that the design is simple in nature as it employs only diodes and variable capacitors, and does not include a feedback-controller circuitry consuming some part of harvested energy.

Implementations of this device are modelled and analyzed, and also simulated. For the design with voltage source, according to simulations on PSpice 11.25μW power can be obtained for $V = 5$V, $C_{max} = 1$nF, $C_{min} = 50$pF, $f = 1$KHz, confirming the theoretical calculations. The macro model experiment is carried out at $V = 40$V, $f = 1$Hz, $C_{max} = 1500$pF, $C_{min} = 45$pF and 22nC charge is gained in every second. The theoretically expected gain is 27nC for the ideal case

where it is assumed that the time constant is zero, diodes are ideal and there is no charge leakage in the circuitry.

An improvement for the capacitors used in energy conversion is also offered. Placing an electret in between the plates of the capacitor and charging this electret, a secondary electric field is created between the plates and this way more charge accumulation is achieved on the outer plates -to compensate for this secondary field. In our design, with this improvement, the power no longer depends strictly on C_{max}, but depends also on the charge trapped on the electret. If large amount of charge is trapped on the electret, then C_{max} value becomes less important and we can work with smaller capacitors; and in this case, the charge gain in every cycle is approximately equal to the amount of trapped charge. We also simulated designs employing this improved capacitors in PSpice; for $V = 5$V, $V_t = 0.4$V, $C_{max} = 1$nF, $\gamma = 20$, $f = 1$KHz, and 20V being applied through the electret, 20.9μC charge gain is obtained in one second. Theoretically, for a circuit without leakage current and employing ideal diodes it was expected to be 21.03μC, and without the electret this circuit would produce 2.03μC charge in one second.

Physical design should compromise mechanical and electrical requirements. The variable capacitors need to be high capacitance in order to circulate high amount of electrical power in the circuit, the mass and its travelling distance should be large for a high quality system sustaining large amount of mechanical energy, spring constant should be small to be able to work at small frequencies where the power content is higher, and also aspect ratio, minimum dimension and fraction limits of the fabrication stage should be considered. The difficulty in matching these conditions altogether decrease the conversion efficiency significantly. The charge embedded capacitor gives more flexibility at physical design stage, and it increases the conversion efficiency for a given volume.

The fabrication of this capacitor-diode system is fully compatible with MEMS technology. The mechanically resonating capacitor is one of the commonly used components in sensor applications that can be produced as a pure silicon device, especially the comb-drive structure is a useful model for us with its tightly placed plates generating high capacitance. We hope to further increase the maximum achievable capacitance value in a limited volume by merging current designs with other technologies such as microfluidics to come up with new capacitor models.

The idea of differentiating the circuit configuration making use of switches can also be applied to other suitable energy converters transducing any form of energy, and the charge embedded capacitor design presented in Chapter 3 can be used with other applications employing capacitors, where it may serve to increase efficiency or solve potential problems.

Bibliography

[1] Jose Oscar Mur Miranda,*Electrostatic Vibration-to-Electric Energy Conversion*, Ph.D. Thesis, Massachusetts Institute of Technology,2004.

[2] Rajeevan Amirtharajah and Anantha P. Chandrakasan, "Self-Powered Signal Processing Using Vibration-Based Power Generation", *IEEE Journal Of Solid-State Circuits*, vol. 33, pp. 687-695, 1998.

[3] R. Amirtharajah, S. Meninger, J.O. Mur-Miranda, A.P. Chandrakasan, J.H. Lang, "A Micropower Programmable DSP Powered Using a MEMS-Based Vibration-to-Electric Energy Converter ", *2000 IEEE International Solid-State Circuits Conference (ISSCC '00)*, pp. 362-363, 2000.

[4] P. D. Mitcheson and T. C. Green and E. M. Yeatman and A. S. Holmes, "Architectures for vibration-driven micro power generators", *IEEE Journal of Microelectromechanical Systems*, vol. 13, pp. 429-440, 2004.

[5] S. Roundy and P. K. Wright and K. S. J. Pister, "Micro-electrostatic vibration-to-electricity converters", *Proceedings of IMECE2002, ASME International Mechanical Engineering Congress and Exposition*, New Orleans, Louisiana, pp. 1-10, 2002.

[6] S. Meninger and J. O. Mur-Miranda and R. Amirtharajah and A. P. Chandrakasan and J. H. Lang, "Vibration-to-electric energy conversion", *IEEE Transactions on VLSI Systems*, vol. 9, pp. 64-76, 2001.

[7] T. Sterken and K. Baert and R. Boers and S. Borghs, "Power extraction from ambient vibration", *Proceedings of Semiconductor Sensors*, Veldhoven, The Netherlands, pp. 680-683, 2002.

[8] R. Tashiro and N. Kabei and K. Katayama and F. Tsuboi and K. Tsuchiya, "Development of an electrostatic generator for a cardiac pacemaker that harnesses the ventricular wall motion", *Japanese Society Journal of Artificial Organs*, vol. 5, pp. 239-245, 2002.

[9] P. Miao and A. S. Holmes and E. M. Yeatman and T. C. Green, "Micro-Machined Variable Capacitors for Power Generation", *Proceedings of Electrostatics 2003*, Edinburgh, UK, 2003.

[10] C. B. Williams, C. Shearwood, M. A. Harradine, P. H. Mellor, T. S. Birch, and R. B. Yates, "Development of an electromagnetic micro-generator", *IEE Proceedings - Circuits, Devices and Systems*, vol. 148, pp. 337-342, 2001.

[11] Wen J. Li, Gordon M. H. Chan, Neil N. H. Ching, Philip H. W. Leong, and Hiu Yung Wong, "Dynamical modeling and simulation of a laser-micromachined vibration-based micro power generator", *International Journal of Nonlinear Sciences and Numerical Simulation*, vol. 1, pp. 345-353, 2000.

[12] P. Glynne-Jones, S. P. Beeby, E. P. James, and N. M. White,"The modelling of a piezoelectric vibration powered generator for microsystems", *Proc. Transducers'01 / Eurosensors XV*, Munich, Germany, pp. 46-49, 2001.

[13] G. K. Ottman, H.F. Hofmann, A.C. Bhatt, and G.A. Lesieutre,"Adaptive piezoelectric energy harvesting circuit for wireless remote power supply", *IEEE Transactions on Power Electronics*, vol. 17, pp.669-676, 2002.

[14] Gideon Gimlan, "Electrostatic Energy Generators and Uses of Same", *U.S. Patent Number 6936994*, applied for Sep 3, 2002, received Aug 30, 2005.

[15] J Andrew Yeh, Chi-Nung Chen and Yen-Seng Lui, "Large rotation actuated by in-plane rotary comb-drives with serpentine spring suspension", *Journal Of Micromechanics And Microengineering*, vol. 15, pp. 201-206, 2005.

[16] Ki-Hun Jeong and Luke P Lee, "A novel microfabrication of a self-aligned vertical comb drive on a single SOI wafer for optical MEMS applications", *Journal Of Micromechanics And Microengineering*, vol. 15, pp. 277-281, 2005.

[17] Vikram Kowshik, Andy Teng-Feng Yu, "Charge Pump", *U.S. Patent Number 5907484*, applied for Aug 25, 1997, received May 25, 1999.

[18] Michael D. Floyd,Jeffrey D. Stump, "Charge Pump Voltage Regulator", *U.S. Patent Number 4807104*, applied for Apr 15, 1988, received Feb 21, 1989.

[19] Jun-ichi Tsujimoto, "Charge Pump Circuit Having a Boosted Output Signal", *U.S. Patent Number 4935644*, applied for Aug 4, 1988, received Jun 19, 1990.

[20] Shadrach Joseph Roundy,*Energy Scavenging for Wireless Sensor Nodes with a Focus on Vibration to Electricity Conversion*, Ph.D. Thesis, The University Of California, Berkeley,2003.

[21] Scott Meninger,*A Low Power Controller for a MEMS Based Energy Converter*, M.S. Thesis, Massachusetts Institute of Technology,1999.

[22] T. Starner and J.A. Paradiso, "Human- Generated Power for Mobile Electronics",*Low-Power Electronics Design*, C. Piguet, ed., CRC Press, chapter 45, pp. 135, 2004.

[23] T. Sterken, K. Baert, R. Puers, G. Borghs, and R. Mertens, "A New Power MEMS Component with Variable Capacitance", *Proc. Pan Pacific Microelectronics Symp.*, pp. 2734, Feb. 2003.

[24] Bernard C. Yen, Jeffrey H. Lang, "A Variable-Capacitance Vibration-to-Electric Energy Harvester", *IEEE Transactions On Circuits And Systems*, vol. 53, pp. 288-295, 2006.

[25] Thomas von Buren, Paul Lukowicz, and Gerhard Troster, "Kinetic Energy Powered Computing - an Experimental Feasibility Study", *Proc. 7th IEEE Int. Symposium on Wearable Computers (ISWC 03)*, pp. 22-24, 2003.

[26] P.D. Mitcheson, B.H. Stark, P. Miao, E.M. Yeatman, A.S. Holmes and T.C. Green, "Analysis and Optimisation of MEMS Electrostatic On-Chip Power Supply for Self-Powering of Slow-Moving Sensors", *Proc. 17th Eur. Conf. Sensors Actuators (Eurosensors03)*, Portugal, pp. 492495, Sep. 2003.

[27] Bernard H. Stark, Paul D. Mitcheson, Peng Miao, Tim C. Green, Eric M. Yeatman, Andrew S. Holmes, "Converter Circuit Design, Semiconductor Device Selection and Analysis of Parasitics for Micropower Electrostatic Generators", *IEEE Transactions On Power Electronics*, vol. 21, pp. 27-37, 2006.

[28] P. Miao, P.D. Mitcheson, A.S. Holmes, E.M. Yeatman, T.C. Green, B.H. Stark, "Mems Inertial Power Generators for Biomedical Applications", *Microsystem Technologies*, vol. 12, pp. 1079-1083, 2006.

[29] M. Miyazaki, H. Tanaka, G. Ono, T. Nagano, N. Ohkubo, T. Kawahara, and K. Yano, "Electric-Energy Generation Using Variable-Capacitive Resonator for Power-Free LSI: Efficiency Analysis and Fundamental Experiment", *ISLPED'03*, Seoul, Korea, pp. 193-198, 2003.

[30] C.B. Williams, R.C. Woods, R.B. Yates, "Feasibility Study of a Vibration Powered Micro-Electric Generator", *IEE Colloquium on Compact Power Sources*, London, UK, pp. 7/1-7/3, 1996.